Application of nature-inspired optimization algorithms to ANFIS model to predict wave-induced scour depth around pipelines

Ahmad Sharafati[1,2,3]*, Ali Tafarojnoruz[4], Davide Motta[5], Zaher Mundher Yaseen[1,6,7]

1. Institute of Research and Development, Duy Tan University, Da Nang 550000, Vietnam.

2. Faculty of Civil Engineering, Duy Tan University, Da Nang 550000, Vietnam

3. Department of Civil Engineering, Science and Research Branch, Islamic Azad University, Tehran, Iran

[4] Dipartimento di Ingegneria Civile, Università della Calabria, Cubo 42B, Rende, Italy

[5] Department of Mechanical and Construction Engineering, Northumbria University, Wynne Jones Building, Newcastle upon Tyne NE1 8ST, United Kingdom

[6] Dams and Water Resources Engineering Department, College of Engineering, University of Anbar, Ramadi 31001, Iraq

[7] School of Civil Engineering, Faculty of Engineering, Universiti Teknologi Malaysia (UTM), 81310 Johor Bahru, Malaysia

Corresponding author: Ahmad Sharafati

Email: ahmadsharafati@duytan.edu.vn

Abstract

Wave-induced scour depth below pipelines is a physically complex phenomenon, whose reliable prediction may be challenging for pipeline designers. This study shows the application of Adaptive Neuro-Fuzzy Inference System (ANFIS) incorporated with Particle Swarm Optimization ($ANFIS-PSO$), Ant Colony ($ANFIS-ACO$), Differential Evolution ($ANFIS-DE$) and Genetic Algorithm ($ANFIS-GA$) and assesses the scour depth prediction performance and associated uncertainty in different scour conditions including live-bed and clear-water. To this end, the non-dimensional parameters Shields number (θ), Keulegan–Carpenter number (KC) and embedded depth to diameter of pipe ratio (e/D) are considered as prediction variables. Results indicate that the $ANFIS-PSO$ model ($R^2_{live-bed}=0.832$ and $R^2_{clear-water}=0.984$) is the most accurate predictive model in both scour conditions when all three mentioned non-dimensional input parameters are included. Besides, the $ANFIS-PSO$ model also shows a better prediction performance than recently developed models. Based on the uncertainty analysis results, the prediction of scour depth is characterized by larger uncertainty in the clear-water condition, associated with both model structure and input variable combination, than in live-bed condition. Furthermore, the uncertainty in scour depth prediction for both live-bed and clear-water conditions is due more to the input variable combination ($R-factor_{ave}=4.3$) than it is due to the model structure ($R-factor_{ave}=2.2$).

Keywords: Pipeline, Wave-Induced Scour, Prediction, Adaptive Neuro Fuzzy Inference System, Optimization Methods, Uncertainty Analysis.

1. Introduction

Submarine pipelines are commonly utilized to carry gas and oil in offshore areas and usually lie on erodible seafloors. Wave action may wash out sediment around a pipeline due to a localized increase of bed shear stress, with consequent development of a scour hole that may undermine the stability of the pipeline and eventually lead to its collapse. In fact, the pipeline may become suspended in seawater as the scour develops, making its structure not able to withstand static and dynamic forces. Pipeline failure not only represents an economic loss but may also cause significant environmental consequences. Thus, consideration of the scour phenomenon beneath offshore pipelines is key during pipeline design (Fredsøe et al. 1988; Yasa and Etemad-Shahidi 2014).

Most of the available predictive scour depth formulas in this context are based on laboratory experiments (Lucassen 1984; Sumer and Fredsøe 1990; Çevik and Yüksel 1999). Such regression-based equations are of straightforward use, and they are commonly adopted to estimate scouring depth around pipelines and, generally, any river or marine structures; however, possible scale effects may lead to considerable inaccuracy in predicting scour for large-scale structures in the field (Tafarojnoruz 2012; Tafarojnoruz and Gaudio 2012). To overcome this limitation, numerical models may be developed for local erosion simulation (Zhao and Fernando 2007; Zhao et al. 2018); such studies, however, are still limited in number and are generally dependent on validation against laboratory observations. Furthermore, simulating scour phenomena with a numerical model is computationally burdensome: resolving a three-dimensional scour hole up to the point it reaches equilibrium may take weeks to months of machine time, which is often impractical for any project's purposes.

Soft Computing (SC) techniques have been increasingly adopted to analyze and predict various hydraulic phenomena. For instance, the use of Group Method of Data Handling (GMDH), applied to the prediction of the longitudinal dispersion coefficient in rivers, offered more accurate estimations compared with the available empirical equations (Najafzadeh and Tafarojnoruz 2016); a study on the calculation of riprap stone size for protection of a steep slope revealed that Evolutionary Polynomial Regression (EPR) is a robust alternative to the empirical mathematical formulations (Najafzadeh et al. 2018); numerous studies demonstrated the capability of Artificial Intelligence (AI) techniques in predicting local scour depth around hydraulic structures (Najafzadeh et al. 2017; Ebtehaj et al. 2018; Najafzadeh and Kargar 2019).

Scour development adjacent to submarine pipelines is generally caused by the shear stress on the seabed associated with waves, currents, or a combination of both. Previous investigations have used AI techniques to predict current-induced, and wave-induced scour depth. For current-induced scouring, the earliest studies focused on Artificial Neural Networks (ANNs)-based and Genetic Programming (GP)-based scour depth prediction around pipelines crossing rivers, producing an acceptable prediction performance (Azamathulla and Ghani 2010; Azamathulla and Zakaria 2011). (Zanganeh et al. 2011) adopted an optimization-based methodology (i.e., PSO algorithm) to mitigate the shortcomings of an Adaptive Neuro Fuzzy Inference System (ANFIS) model for current-induced scour prediction. (Yasa and Etemad-Shahidi 2014) derived scour prediction formulations for live-bed and clear-water-scour conditions by combining the Model Tree (MT) and regression model.

Utilizing some of the AI methods may lead to derive new prediction equations. These equations may generally have a more complicated mathematical structure than those resulting from the conventional regression-based approaches, but at the same time may offer more accurate

predictions. For instance, (Najafzadeh and Sarkamaryan 2018) proposed Gene-Expression Programming (GEP), EPR and MT algorithms to extract mathematical formulations for estimating current-induced scour depth below pipelines. Recent studies showed the capabilities of Multivariate Adaptive Regression Splines and Support Vector Machine techniques in predicting scour depth under pipelines in rivers (Haghiabi 2017, 2019; Parsaie et al. 2019).

For wave-induced scour, the prediction performance of an ANN approach, one of the most common AI models, was assessed in comparison with regression-based formulations (Kazeminezhad et al. 2010). Although this study reported accurate predictions using the ANN approach, its application is not easy to carry out by engineers. To overcome this limitation, a Model Tree (MT) was later developed to derive more easily usable predictive equations (Etemad-Shahidi et al. 2011). These studies, as well as other application of different AI approaches, e.g. GMDH (Najafzadeh et al. 2014a, b), demonstrate the feasibility of SC models to estimate the scour depth caused by waves or currents around submarine pipelines. In particular, the combination of two AI techniques has shown to enhance prediction performance: for instance, a GMDH network programmed using a GEP technique provided excellent prediction results for scouring under pipelines (Najafzadeh and Saberi-Movahed 2018).

A common AI approach, ANFIS, combines ANN and Fuzzy Inference System (FIS) and is widely used to estimate scouring depth around hydraulic structures. Because of the flexibility provided by ANNs, ANFIS models can get trained following a complex mathematical mapping between inputs and outputs within a nonlinear framework. Moreover, the 'IF and THEN' rules, embedded in FIS, allow for forecasting the behavior of uncertain systems. In recent years, ANFIS models have been applied to estimate the scouring depth at bridge piers and abutments (Akib et al. 2014; Choi et al. 2017; Moradi et al. 2018), culvert outlets (Azamathulla and Ghani 2011) and long contractions

along straight canals (Najafzadeh et al. 2016). It can be therefore expected that the ANFIS technique can satisfactorily be used for prediction of scour around pipelines as well.

Recently, the nature-inspired algorithms, i.e., Ant Colony Optimization (ACO), Particle Swarm Optimization (PSO), Differential Evolution (DE), and Genetic Algorithm (GA) have been introduced for optimization purposes in various engineering problems. Specifically to water resources engineering, for instance, ACO algorithm has been used to analyze optimal groundwater long-term strategies (Li and Chan Hilton 2005, 2007); PSO algorithm has been adopted to optimize water distribution networks (Surco et al. 2018), rainfall-runoff forecasting models (Motahari and Mazandaranizadeh 2017) and scour depth estimations (Zanganeh et al. 2011; Najafzadeh 2015).

The progression of AI modeling in the field of hydraulic engineering indicates the limitations of the existed AI models and the enthusiasm for solving those limitations. The primary contribution of the present study is to address the internal tuning parameters that are associated with the ANFIS model. This has been scientifically evidenced over the recent literature, and thus the main motivation of the methodological phase is taken place.

The goal of this study is to enhance the capability of the ANFIS technique to estimate scouring depth under submarine pipelines by combining it with the aforementioned nature-inspired optimization algorithms. The prediction accuracy of the proposed methodology is then quantified and compared with the most recent formulations obtained with stochastic approaches for wave-induced pipeline scour depth (Etemad-Shahidi et al. 2011; Sharafati et al. 2018) using indices of prediction performance.

2. Governing variables and scour depth prediction formulations

Pipeline failure may occur because of various reasons. Inadequate cover or a low specific gravity of the pipeline may both result in pipeline deterioration and eventual failure; therefore, they must be considered when designing and laying a pipeline. The focus of this investigation is bed scour, which is another possible cause of pipeline failure. The scouring process around any marine or river structure is a complex phenomenon, and various physical factors affect its development. Several governing variables regarding water, pipeline and seabed interaction are typically considered when predicting scour depth. Previous studies (Sumer and Fredsøe 1990; Kazeminezhad et al. 2010; Najafzadeh et al. 2014a) showed that the variables affecting the wave-induced scour under a pipeline are mainly related to the fluid (herein water), flow regime, seabed sediment and pipeline properties. In general, the maximum equilibrium scour depth at a submarine pipeline, S, may be expressed with the following unknown functional relationship, f_1:

$$S = f_1(\rho, \rho_s, g, D, d_{50}, U_m, u_{*w}, T, e, H, \mu) \quad (1)$$

where ρ and ρ_s are water and sediment mass densities, g is the acceleration of gravity, D is the pipe diameter, d_{50} is the median diameter of the sediment particles; U_m, u_{*w} and T are, respectively, the maximum magnitude of the undisturbed orbital fluid velocity at the bed, wave friction velocity and wave period, respectively; e, H and μ denote the gap between the pipeline and the initial bed, wave height and dynamic viscosity of water, respectively. Among the parameters within the above equation, U_m and T represent the wave characteristics for any wave-induced scour condition around a pipeline.

Through dimensional analysis, the above relationship can be rewritten in terms of dimensionless parameters. For the case of a pipeline with a smooth outer surface (Najafzadeh et al. 2014a):

$$S/D = f_2(R, R_d, e/D, \theta, KC) \quad (2)$$

where f_2 is an unknown function, R and R_d represent Reynolds number and sediment grain Reynolds number, respectively, which are expressed as

$$R = \frac{\rho U_m D}{\mu} \tag{3}$$

$$R_d = \frac{\rho u_{*w} d_{50}}{\mu} \tag{4}$$

and the Shields number, θ, and the Keulegan–Carpenter number, KC, are expressed as

$$\theta = \frac{{u_{*w}}^2}{\left(\frac{\rho_s}{\rho} - 1\right) g d_{50}} \tag{5}$$

$$KC = \frac{U_m T}{D} \tag{6}$$

Both KC and R depend on the flow field close to the pipeline, whereas R_d and θ also take into account the seabed characteristics. Because of the relationship of the Reynolds number parameters, i.e. R and R_d, with the dimensionless variables θ and KC and the typical existence of turbulent flow field conditions around pipelines, the Reynolds number parameters can be neglected and Eq. (2) is simplified as in the following functional relationship with unknown function f_3 (Kazeminezhad et al. 2010; Etemad-Shahidi et al. 2011; Najafzadeh et al. 2014a; Sharafati et al. 2018):

$$S/D = f_3(e/D, \theta, KC) \tag{7}$$

Among the dimensionless parameters in the above equation, the magnitude of KC plays a critical role in the resulting maximum scour depth (Lucassen 1984; Sumer and Fredsøe 1990). The influence is so notable that (Çevik and Yüksel 1999) proposed a simple scour depth prediction equation based on KC as the only effective parameter on S/D, where no gap exists between the pipeline and the bed:

$$\frac{S}{D} = 0.11KC^{0.45} \tag{8}$$

Although for the estimation of maximum scour depth beneath a pipeline placed above the seabed level other researchers (Sumer and Fredsøe 2002; Mousavi et al. 2009) derived predictive formulas neglecting θ, a more accurate scour depth estimation is obtained if all the dimensionless parameters in Eq. (7) are included. To this end, based on a MT approach, (Etemad-Shahidi et al. 2011) derived a set of mathematical formulations to predict the scouring depth by considering all the parameters in Eq. (7).

Recently, Sharafati et al. (2018) revised the coefficients and exponents of Etemad-Shahidi et al. (2011)'s formulations, assuming that the uncertainty associated with the dataset they utilized is the primary source of the variability of the parameters. The uncertainty analysis was performed using two stochastic approaches: Generalized Likelihood Uncertainty Estimation (GLUE) and Sequential Uncertainty Fitting (SUFI). Based on the GLUE method, which provided more accurate results than SUFI, Sharafati et al. (2018) proposed the following formulae for clear-water (Eq. 9) and live-bed scour conditions (Eq. 10):

$$\frac{S}{D} = 4.17\ KC^{0.72}\theta^{1.55} \exp\left(-3.9\ {}^{e}/_{D}\right)\ \ for\ \ \theta \leq 0.064 \tag{9}$$

$$\frac{S}{D} = \begin{cases} 0.149KC^{0.42}\theta^{0.08} \exp\left(-0.472\ {}^{e}/_{D}\right) & for\ \ \theta > 0.064\ \ and\ \ {}^{e}/_{D} \leq 0.145 \\ 0.073KC^{0.45}\theta^{0.17} \exp\left(-0.094\ {}^{e}/_{D}\right) & for\ \ \theta > 0.064\ \ and\ \ {}^{e}/_{D} > 0.145 \end{cases} \tag{10}$$

Equations (9) and (10) are the latest and most comprehensive equations for estimation of wave-induced ultimate scour depth beneath pipelines. In the present investigation, predictions obtained with the new proposed methodology are compared with the results of these equations, as well as the equations by Etemad-Shahidi et al. (2011). The prediction improvement provided by the new

model is discussed, and the uncertainty due to the input parameters and the model structure is assessed in detail.

3. Proposed hybrid artificial intelligence models

The recent years have seen a noticeable advancement of SC approaches (Sharafati et al. 2019). Such methods are suitable for solving complex problems characterized by a high level of non-linearity and non-stationarity (Yaseen et al. 2015). Hybridized AI-global optimization models have recently gained popularity (Ghorbani et al. 2017). Among them, the performance of nature bio-inspired models has been the best owing to the AI models-associated hyper-parameters (Maier et al. 2014).

This study hybridized four nature bio-inspired algorithms, namely PSO, ACO, DE and GA, with an ANFIS model for wave-induced maximum scour depth prediction at pipelines. Figure 1 outlines the developed models in the form of flowcharts.

[Fig 1]

3.1.ANFIS model

ANFIS models are very well-established AI models based on fuzzy logic (Jang 1996) and their popularity is because they allow input variables (attributes) to execute numerical approximation of the internal mechanism relationships of a physical phenomenon (Yaseen et al. 2017). In essence, ANFIS models boost the learning capability of a classic ANN, which develops rules to map a set of inputs to an output value based on a set of fuzzy rules presented by Zadeh (1965). The fuzzy logic component is exceptionally beneficial as it aids in optimal solution generation (in terms of prediction performance) from imprecise/noisy input attributes.

The fuzzy logic approach is based on allowing each element of a dataset to fall in a particular class (set) partially, and its membership degree is described by a membership function. Achieving an accurate learning process based on knowledge and appropriate related experience requires optimal selection of the shape of the membership functions, knowledge and fuzzy rules (Kisi and Yaseen 2019).

The general five-layer structure of an ANFIS model is illustrated in Figure 2, describing the case of two input parameters and an output variable. The ANFIS rules are expressed through the following 'if' and 'then' functions:

$$\text{Rule \#1: } If\ x\ is\ A_1\ and\ y\ is\ B_1, then\ f_1 = p_1x + q_1y + r_1 \tag{11}$$

$$\text{Rule \#2: } If\ x\ is\ A_2\ and\ y\ is\ B_2, then\ f_2 = p_2x + q_2y + r_2 \tag{12}$$

where (A_1&A_2) and (B_1&B_2) are linguistic terms of the inputs x and y, and p_1, q_1, r_1, p_2, q_2, r_2 are coefficients of linear equations.

[Fig 2]

Within the first layer of the model, each node is considered as an adaptive node with the following node function

$$\text{For input } x\text{:} \quad O_{1,i} = \mu_{A_i}(x), \qquad i = 1,2 \tag{13}$$

$$\text{For input } y\text{:} \quad O_{1,i} = \mu_{B_i}(y), \qquad i = 1,2 \tag{14}$$

where the subscript "1" stands for "the first layer", x or y represents the input value to the node i and μ_{A_i} and μ_{B_i} denote the membership functions representing the linguistic term A_i (for input

value x) and B_i (for input value y), respectively. Various types of membership functions have earlier been reported in the literature, such as trapezoidal, Gaussian, and triangular; however, this study adopted the Gaussian function, which is expressed thus:

$$\mu_{A_i}(x) = \exp\left(-\left(\frac{x - a_i}{b_i}\right)^2\right) \tag{15}$$

$$\mu_{B_i}(x) = \exp\left(-\left(\frac{y - c_i}{d_i}\right)^2\right) \tag{16}$$

where a_i, b_i, c_i and d_i, are distribution variables.

The second model layer has each node fixed while the model output is computed as

$$O_{2,i} = W_i = \mu_{A_i}(x) * \mu_{B_i}(y), \qquad i = 1,2 \tag{17}$$

where the subscript "2" stands for "second layer" and W_i are the rules' weights.

Within the third layer of the model, each node computes the ratio of the corresponding rule weight and the sum of the weights as follows:

$$O_{3,i} = \overline{W_i} = \frac{W_i}{W_1 + W_2}, \qquad i = 1,2 \tag{18}$$

In the fourth layer, each node is adaptive, and the output is computed as

$$O_{4,i} = \overline{W_i} f_i = \overline{W_i}(p_i x + q_i y + r_i), \qquad i = 1,2 \tag{19}$$

where $\overline{W_i}$ stands for the third layer output and the coefficients p_i, q_i and r_i are updated during the training based on the training set.

In the fifth layer (the final one), the circulation of the nodes is carried out as follows:

$$O_5 = \sum_{i=1,2} \overline{W_i} f_i = \frac{\sum_i W_i f_i}{\sum_i W_i} \tag{20}$$

3.2.*Optimization algorithms*

The optimization of the rules that map the inputs to an output value is typically done with trial and error procedures and the ANFIS model utilizing this type of optimization is referred to as 'classic' ANFIS model. Such trial and error procedures have the disadvantage of often being time-consuming and can lead to overfitting. These issues can be mitigated by using global optimization algorithms. The methodologies for optimization used in this investigation are outlined in the following sub-sections.

3.2.1. Particle Swarm Optimization (PSO) algorithm

The PSO technique is a bio-based optimizer first introduced by Eberhart & Kennedy (1995); it was inspired by the pattern of movement of natural creatures like such as fish, insects, and birds. This methodology models each candidate solution to an optimization problem as a particle flowing in the search domain of the optimization problem. The location (position) and speed of every single particle are adjusted following its own experience and the neighboring particles.

The formulation to update the location of particle *i* is

$$P_i^{t+1} = P_i^t + V_i^{t+1} \tag{21}$$

where P_i^{t+1} is the position of the particle at time t+1 and and P_i^t is the position of the particle at time t; V_i^{t+1} is the velocity of the particle at time t+1, which is updated thus

$$V_i^{t+1} = V_i^t + c_1 U_1^t (PB_i^t - P_i^t) + c_2 U_2^t (GB_i^t - P_i^t) \quad (22)$$

where V_i^t is the particle velocity at time t, c_1 and c_2 are acceleration coefficients, U_1^t and U_2^t are random values varying between 0 and 1, and PB_i^t is the personal best position while GB_i^t is the global best position, in optimization terms, of the i^{th} particle at time t. The parameters used for the application of the PSO optimization technique are summarized in Table 1.

3.2.2. Ant Colony Optimization (ACO) algorithm

The ACO was first presented by Dorigo & Di Caro (Dorigo and Di Caro 1999) as an optimizer which has undergone several modifications to suit multiple engineering applications (Weise 2009; Afshar et al. 2015; Ajay Adithyan et al. 2018). The ACO algorithm is an optimization technique that is most effective in addressing both dynamic and static problems in the field of engineering (Dorigo et al. 1996; Blum 2005; Dorigo and Blum 2005; Dorigo and Socha 2007).

Although colonies of ants are composed of simple individuals, they are considered to have one of the most well-organized structures in nature (Guo and Zhu 2012). The stigmergy mechanism which facilitates self-organization controls activities like foraging, brood sorting, co-operative transport, and division of labor (Dorigo and Di Caro 1999). Stigmergy in ant colonies is based on the pheromone track left by each ant, which affects the actions of all the other ants. The ACO algorithm, inspired by this concept, can find the best solution in an optimization problem through forward & backward movements, as well as a step-wise decision process. The parameters used for the application of the ACO optimization technique are summarized in Table 1.

3.2.3. Differential Evolution (DE) algorithm

The DE methodology is a stochastic nature-inspired framework for solving problems that are considered highly nonlinear & multi-dimensional (Suribabu 2010; Chen and Chau 2016); it was first proposed by Storn and Price (Storn and Price 1995). The optimization of a function with population size *k* and *n* real variables first requires the formulation of the vectors in the following manner:

$$x_{i,G} = [x_{1,i,G}, x_{2,i,G}, \ldots x_{n,i,G}] \qquad i = 1, 2, \ldots, k \tag{23}$$

where *G* represents the number of generations. Each parameter has an upper & lower boundary defines as follows:

$$x_j^L \leq x_{j,i,1} \leq x_j^U \tag{24}$$

Therefore, identity probability is invoked in setting the initial magnitudes of the variables. The parameters used for the application of the DE optimization technique are summarized in Table 1.

3.2.4. Genetic Algorithm (GA)

GA algorithm is an evolution-based algorithm that was developed based on the Darwins principle of natural selection for addressing numerous optimization problems (Yang and Honavar 1998; Maulik and Bandyopadhyay 2000; Deb et al. 2002; Levasseur et al. 2008; Iba and Aranha 2012; Kubat 2017)(Koza 1994). The algorithm is initialized by generating an initial random population of individual solutions to the considered problem. The goodness of fit for each solution is then assessed using suitable metrics, and crossover and mutation operators are employed to generate the next generation of individual solutions and allow the population to evolve towards an optimal solution. The parameters used for the application of the GA optimization technique are summarized in Table 1.

[Table 1]

3.2.5. Optimization of parameters

For live-bed conditions, two Gaussian and two linear functions are defined as the membership functions of the input and output variables, respectively. For clear-water conditions, one Gaussian and one linear function are defined as membership functions of the input and output variables, respectively. For instance, for a combination of three input variables, the total number of parameters to be optimized is 20 (12 antecedent – input-related – parameters and 8 consequent – output-related – parameters) for live-bed conditions and 10 (6 antecedent parameters and 4 consequent parameters) for clear-water conditions. The number of membership functions employed in this study is selected based on the available number of data for the training phase, and the number of parameters to optimize is less than the number of training data. Table 2 shows an example of optimized parameters for the ANFIS-PSO model with three input variables.

[Table 2]

3.3.Description of the proposed predictive models

Several combinations of input variables ($\frac{e}{D}, \theta \; and \; KC$) are considered to identify the optimal predictive model for wave-induced pipeline scour depth under live-bed as well as clear-water conditions. Individually, seven input combinations, called $M1$ to $M7$, are evaluated (Table 3). In total, 35 different predictive models are assessed, employing different predictive approaches ($ANFIS, ANFIS-PSO, ANFIS-ACO, ANFIS-DE$ and $ANFIS-GA$) and different input variable combinations ($M1$ to $M7$).

[Table 3]

4. Dataset for the analysis

To develop the mentioned AI models, laboratory experimental datasets with a total of 69 scour depth observations from four sources are collected (Lucassen 1984; Sumer and Fredsøe 1990; Pu et al. 2001; Mousavi et al. 2009). The datasets are deemed suitable for the present study because of the following: all the datasets were collected for conditions characterized by $KC < 100$, which imply the pipelines were exposed to the wind wave, the pipe surface was hydraulically-smooth, and the current induced by waves was perpendicular to the pipe; the experiments were performed under a wide range of Reynolds numbers, reproducing field conditions; and the channel width in all the tests was large enough to neglect the influence of sidewalls.

The analysis is performed separately for clear-water (21 observations), and live-bed (48 observations) scour conditions. The training-testing data are provided based on the 31-17 (in live-bed condition) and 13-8 (in clear-water condition) observations. The data division adopted between training and testing phases is the result of a trial and error search to attain the best performance. Table 4 summarizes the statistical characteristics of the dimensionless parameters e/D, θ, KC and S/D for the overall dataset considered; the range of variation of the parameters is wide enough to obtain robust results.

[Table 4]

5. Indices of prediction performance

Four different indices, i.e. Root Mean Square Error ($RMSE$) (Salih et al. 2019, 2020), Mean Absolute Error (MAE)(Hai et al. 2020), Correlation of determination (R^2) (Sharafati et al. 2020a) and Willmott's Index (WI) (Malik et al. 2020; Mohammed et al. 2020), are computed to measure

the adequacy of the predictive models for wave-induced pipeline scour depth. The indices are calculated as follows:

$$RMSE = \sqrt{\frac{1}{N_T}\sum_{j=1}^{N_T}\left(\left(\frac{S}{D}\right)_{Obs,j} - \left(\frac{S}{D}\right)_{Sim,j}\right)^2} \tag{25}$$

$$MAE = \frac{1}{N_T}\sum_{j=1}^{N_T}\left|\left(\frac{S}{D}\right)_{Obs,j} - \left(\frac{S}{D}\right)_{Sim,j}\right| \tag{26}$$

$$R = \frac{\sum_{j=1}^{N_T}\left(\left(\frac{S}{D}\right)_{Obs,j} - \overline{\left(\frac{S}{D}\right)_{Obs,j}}\right)\left(\left(\frac{S}{D}\right)_{Sim,j} - \overline{\left(\frac{S}{D}\right)_{Sim,j}}\right)}{\sqrt{\sum_{j=1}^{N_T}\left(\left(\frac{S}{D}\right)_{Obs,j} - \overline{\left(\frac{S}{D}\right)_{Obs,j}}\right)^2 \sum_{j=1}^{N_T}\left(\left(\frac{S}{D}\right)_{Sim,j} - \overline{\left(\frac{S}{D}\right)_{Sim,j}}\right)^2}} \tag{27}$$

$$WI = 1 - \left[\frac{\sum_{i=1}^{N_T}\left(\left(\frac{S}{D}\right)_{Obs,j} - \left(\frac{S}{D}\right)_{Sim,j}\right)^2}{\sum_{i=1}^{N_T}\left(\left|\left(\frac{S}{D}\right)_{Sim,j} - \overline{\left(\frac{S}{D}\right)_{Obs,J}}\right| + \left|\left(\frac{S}{D}\right)_{Obs,j} - \overline{\left(\frac{S}{D}\right)_{Obs,J}}\right|\right)^2}\right] \tag{28}$$

where $\left(\frac{S}{D}\right)_{Obs}$ and $\left(\frac{S}{D}\right)_{Sim}$ are observed and predicted non-dimensional scour depth magnitudes, respectively, while $\overline{\left(\frac{S}{D}\right)_{Obs}}$ is the observed non-dimensional scour depth mean magnitude while and $\overline{\left(\frac{S}{D}\right)_{Sim}}$ is the predicted non-dimensional scour depth mean magnitude. N_T stands for the number of considered datasets. The smaller $RMSE$ or MAE, or the closer to 1.0 R^2 or WI are, the better the prediction performance.

To quantify the performance improvement offered by the ANFIS models optimized using the nature-inspired algorithms compared with the classic ANFIS model, the Improvement Index (*IM*) is calculated in the testing stage (Sharafati et al. 2020b) as follows:

(29)

$$IM_{test} = \frac{\left(IM_{test}^{RMSE} + IM_{test}^{MAE} + IM_{test}^{R^2} + IM_{test}^{WI}\right)}{4}$$

where

$$IM_{test}^{RMSE} = \frac{\left(RMSE_{test}^{\text{ANFIS}} - RMSE_{test}^{Model}\right)}{RMSE_{test}^{\text{ANFIS}}} \times 100 \quad (30)$$

$$IM_{test}^{MAE} = \frac{\left(MAE_{test}^{\text{ANFIS}} - MAE_{test}^{Model}\right)}{MAE_{test}^{\text{ANFIS}}} \times 100 \quad (31)$$

$$IM_{test}^{R^2} = \frac{\left(R^{2}{}_{test}^{Model} - R^{2}{}_{test}^{\text{ANFIS}}\right)}{R^{2}{}_{test}^{\text{ANFIS}}} \times 100 \quad (32)$$

$$IM_{test}^{WI} = \frac{\left(WI_{test}^{Model} - WI_{test}^{\text{ANFIS}}\right)}{WI_{test}^{\text{ANFIS}}} \times 100 \quad (33)$$

where, $RMSE_{test}^{\text{ANFIS}}$, $MAE_{test}^{\text{ANFIS}}$, $R^{2}{}_{test}^{\text{ANFIS}}$, and WI_{test}^{ANFIS} are, respectively, the computed $RMSE$, MAE, R^2, and WI for the classic ANFIS model, while $RMSE_{test}^{Model}$, MAE_{test}^{Model}, $R^{2}{}_{test}^{Model}$, and WI_{test}^{Model} are the computed indices for the models optimized using the nature-inspired algorithms, for the testing stage.

6. Uncertainty analysis

In this study, two sources of uncertainty attributable to the model structure and the input variables are investigated. To quantify the uncertainty of the model structure, a set of five predicted scour depth values in the testing phase (i.e., predicted set by the aforementioned hybridized models) is assigned to each observed scour depth. For each predicted set, the mean and standard deviation are computed to describe a normal distribution function. Using this distribution, 1000 scour depth

values are generated through the 'Monte Carlo' simulation (MCS) technique. The MCS technique generally quantifies the uncertainty associated with random variables based on their Probability Density Functions (PDFs). A set of input variables is generated in each iteration to simulate a system (model). Then, the model outputs are generated randomly based on the obtained stochastic input variables. This process is repeated for an appropriate number of iterations to achieve a reliable description of the output variability due to the different predictive models adopted (Sharafati and Zahabiyoun 2014; Sharafati and Azamathulla 2018). Recent studies on scouring have used the MCS technique to quantify model output uncertainty, confirming this technique as a robust method to assess the uncertainty associated with scouring prediction (Khalid et al. 2019; Salamatian and Zarrati 2019; Homaei and Najafzadeh 2020; Wu and Luo 2020). To quantify the uncertainty of scour depth prediction, the 95% prediction confidence interval (i.e., the interval between the 97.5% and the 2.5% quantiles), called the '95 percent prediction uncertainty' (95 PPU), is extracted using the generated scour depths for each observed scour depth. Individually, the uncertainty is measured using the $R-factor$ index as follows (Sharafati and Azamathulla 2018):

$$R-factor=\frac{dx}{\sigma x} \tag{34}$$

where σx denotes the standard deviation of the observed data and *dx* is computed as follows

$$dx=\sum_{i=1}^{k}(U_L^i-L_L^i)/k \tag{35}$$

where k stands for the number of observed data and U_L^i and L_L^i denote the i^{th} value of upper quantile (i.e., 97.5%) and lower quantile (i.e., 2.5%) of the 95 PPU band, respectively. This procedure for computation of the $R-factor$ index is carried out in this study for both live-bed and clear-water scour conditions.

To evaluate the uncertainty associated with the input variables, for each observed scour depth, the predicted scour depth is computed in the testing phase for a single model but multiple input combinations ($M1$ to $M7$). Then, the uncertainty associated with the input variables is quantified using the same $R-factor$ approach described above for the uncertainty related to the model structure. Again, this procedure is carried out for both live-bed and clear-water conditions.

7. Results and Discussion

7.1. Assessment of the proposed predictive models

This study examines several ANFIS models hybridized with the different nature-inspired algorithms presented above. Each model uses a different tuning process to obtain the appropriate ANFIS model parameters. Hence, the models provide different prediction performances based on their tuning processes. Comparing the performance metrics of the models is a way to assess the impact of their tuning processes on prediction performance. Specifically, to analyze the prediction performance of the mentioned 35 different predictive models ($ANFIS, ANFIS-PSO, ANFIS-ACO, ANFIS-DE$ and $ANFIS-GA$ for the input combinations $M1$ to $M7$), the selected prediction performance indices ($RMSE, MAE,\ R^2\ and\ WI$) are computed for training, and testing phases and live-bed or clear-water scour conditions (Tables 5-9).

[Table 5-9]

Considering only the classic ANFIS model (see Table 5), $ANFIS-M5$ exhibits the best

prediction performance for live-bed conditions ($R^2{}_{train} = 0.955$, $RMSE_{train} = 0.025$ for training and $R^2{}_{test} = 0.568$, $RMSE_{test} = 0.058$ for testing) among all ANFIS prediction models. For the clear-water conditions, no clearly preferable ANFIS model emerges in training and testing phases, although $ANFIS - M4$ ($R^2{}_{train} = 0.998$, $RMSE_{train} = 0.013$ for training and $R^2{}_{test} = 0.391$, $RMSE_{test} = 0.116$ for testing) shows the best performance. For both the clear-water and live-bed scour conditions, predictions with higher accuracy are resulted from the training phase than the testing phase. Overall, the classic ANFIS model is not robust enough to predict wave-induced scour around the pipelines.

Table 6 indicates that the $ANFIS - PSO$ model offers more accurate predictions than the classic ANFIS model and the best prediction performance among all models considered. In particular, $ANFIS - PSO - M7$ shows the best prediction performance for both live-bed conditions ($R^2{}_{train} = 0.957$, $RMSE_{train} = 0.024$ for training and $R^2{}_{test} = 0.832$, $RMSE_{test} = 0.032$ for testing) and clear-water conditions ($R^2{}_{train} = 0.999$, $RMSE_{train} = 0.0048$ for training and $R^2{}_{test} = 0.984$, $RMSE_{test} = 0.014$ for testing).

Tables 7-9 (relative to ANFIS-ACO, ANFIS-DE and ANFIS-GA) show that the input variable combination that results in the best prediction performance is different for live-bed and clear-water conditions. The $ANFIS - ACO - M7$ ($R^2{}_{test} = 0.324$), $ANFIS - DE - M5$ ($R^2{}_{test} = 0.623$) and $ANFIS - GA - M5$ ($R^2{}_{test} = 0.559$) models are the best performing models for live-bed conditions, whereas the $ANFIS - ACO - M5$ ($R^2{}_{test} = 0.71$), $ANFIS - DE - M7$ ($R^2{}_{test} = 0.692$) and $ANFIS - GA - M7$ ($R^2{}_{test} = 0.433$) models are the best performing models for clear-water conditions.

It must be noted that Tables 5-9 include both error indices (e.g., RMSE and MAE) and similarity

indices (e.g., R^2 and WI). For instance, the ANFIS-M1 model in live-bed conditions results in 0.072, 0.048, 0.623 and 0.876 for RMSE, MAE, R^2 and WI, respectively, in the training phase, and 0.077, 0.054, 0.043, 0.552, respectively, in the testing phase (Table 5). It can, therefore, be observed that the prediction performance is reduced in testing phase by 6.94%, 12.50%, 93.10% and 36.99%, judging respectively from RMSE, MAE, R^2 and WI. This means that, for the case of the ANFIS-M1 model, the prediction performance based on the error indices is reduced from training to testing phase less significantly than the prediction performance based on the similarity indices. For the ANFIS-M5 and ANFIS-M7 models, instead, the error indices show a more significant prediction performance reduction than the similarity indices. This behavior excludes an issue of overfitting in our approach because overfitting would produce the same pattern of prediction performance reduction for the testing phase in both error and similarity indices. The low prediction performance indices, when observed in the testing phase, reflect instead the limitations associated with the dataset sample size and the prediction capability of the model considered. For the best predictive model, ANFIS-PSO-M7, the prediction performance reduction from training to testing phase is quantified, using the RMSE and MAE indices, by a decrease in performance of 25% and 30.8%, respectively (in live-bed conditions), and a decrease of 65.7% and 75.8%, respectively (in clear-water conditions). Considering the R^2 and WI indices, the decrease in performance is 15% and 7.2%, respectively, in live-bed conditions, and 1.6% and 0.49%, respectively, in clear-water conditions. Overall, the error metrics (RMSE and MAE) obtained in testing phase indicate a moderate prediction performance reduction (49.3%), while for the similarity metrics (R^2 and WI) the reduction (6.1%) is negligible.

Our findings indicate that the classic ANFIS model is not accurate in predicting the wave-induced scour depth around pipelines, especially in clear-water conditions ($R^2 = 0.39$ for testing phase) for

which the models ANFIS-PSO (R^2 =0.98), ANFIS-ACO (R^2 =0.71), and ANFIS-DE (R^2 = 0.69) provide a significantly better prediction performance, as a result of the nature-inspired optimization algorithms introduced in this research for the ANFIS model.

The best prediction performance indices for each model in the testing phase is presented in Table 10.

As mentioned, the $ANFIS-PSO$ model with the input variable combination $M7$ (all the three variables, $\frac{e}{D}, \theta \; and \; KC,$ included) is the model resulting in the best prediction performance for both live-bed and clear-water conditions. Furthermore, the obtained IM values (also shown in Table 10) quantify the significant improvement in prediction provided by all the ANFIS models optimized using the nature-inspired algorithms compared with the classic ANFIS model for both live-bead and clear-water conditions in the testing phase, with the most significant improvement obtained with the ANFIS-PSO model ($IM_{Live-bed} = 35\%$ and $IM_{Clea-water} = 90\%$, for testing phase).

[Table 10]

A visual performance comparison between the different models is provided in the heat map in Figure 3, based on the standardized $RMSE, MAE, \; R^2$, and WI performance indices. The RMSE and MAE indices are standardized using the formula ($\frac{X_{max}-X}{X_{max}-X_{min}}$), while the R^2 and WI indices are standardized using the formula ($\frac{X-X_{min}}{X_{max}-X_{min}}$), where X is the index value. The resulting standardized values are therefore within the range 0 to 1 with the best index value having a standardized value of 1. As mentioned, the model $ANFIS-PSO-M7$ (dark blue column) has the best performance indices for both live-bed and clear-water conditions. In contrast, $ANFIS-ACO-M7$ and

$ANFIS - M4$ (red columns) offer the lowest performance for live-bed and clear-water conditions, respectively.

[Fig. 3]

The prediction performance is also evaluated on two-dimensional scatter plots comparing the simulated and the observed values of scour depth (Figure 4), where the identity (1:1) line is a reference to visualize how close the simulated and observed values are. For live-bed conditions (Figure 4a), the $ANFIS - PSO - M7$ points are generally the closest to the 1:1 line and show the most linear pattern (coefficient of determination $R^2 = 0.832$), whereas the points corresponding to the other models are noticeably more scattered ($R^2 = 0.324 \sim 0.623$). Likewise, for clear-water conditions, the $ANFIS - PSO - M7$ points are the nearest to the 1:1 line with $R^2 = 0.984$, whereas most of the points for the other models suggest overestimation of the predicted scour depth.

[Fig. 4]

Models are also comparatively assessed on a Taylor diagram (Figure 5), considering RMSE, R and normalized standard deviation (Taylor 2001). Again, in the diagram the model with the best predictions (i.e., the closest points to the points labeled "observed") is the $ANFIS - PSO - M7$ for both live-bed and clear-water scour conditions.

[Fig. 5]

The variability of the measured and predicted scour depth magnitudes is quantified and compared for the different models by computing and plotting the quantiles $Q_{25\%}$, $Q_{50\%}$ and $Q_{75\%}$ (Figure 6). The median scour depth predicted by the $ANFIS - PSO - M7$ model is the closest to the median

observed value for both live-bed conditions ($Q_{50\%,observed} = 0.24, Q_{50\%,ANFIS-PSO-M7} = 0.23$) and clear-water conditions ($Q_{50\%,observed} = 0.11, Q_{50\%,ANFIS-PSO-M7} = 0.14$). From a comparison of the interquartile range (IQR), which is the difference between $Q_{75\%}$ and $Q_{25\%}$, it appears that the predictive models underestimate the variability of the observed data in live-bed conditions. In contrast, they either under- or overestimate the measured values in clear-water conditions.

[Fig. 6]

7.2. Comparison of the proposed predictive models with the available models in the literature

Besides assessing the performance of the proposed models against observed values of scour depth, a comparison with other recently developed methodologies from literature is carried out. Specifically, two recent studies are considered (Etemad-Shahidi et al. 2011; Sharafati et al. 2018). Etemad-Shahidi et al. (2011) proposed several MT-based equations to predict wave-induced scour depth beneath pipelines in clear-water (Eq. 36) and live-bed (Eqs. 37 and 38) conditions as follows:

$$\frac{S}{D} = 3.344KC^{0.512}\theta^{1.296}exp\left(-2.32\,{}^{e}/_{D}\right) \quad for \quad \theta \leq 0.064 \tag{36}$$

$$\frac{S}{D} = 0.149KC^{0.477}\theta^{0.121}exp\left(-0.472\,{}^{e}/_{D}\right) \quad for \quad \theta > 0.064 \ and \ {}^{e}/_{D} \leq 0.145 \tag{37}$$

$$\frac{S}{D} = 0.048KC^{0.782}\theta^{0.121}exp\left(-0.942\,{}^{e}/_{D}\right) \quad for \quad \theta > 0.064 \ and \ {}^{e}/_{D} > 0.145 \tag{38}$$

Sharafati et al. (2018) improved Etemad-Shahidi et al. (2011)'s equations using the stochastic GLUE and SUFI approaches and developed Eqs. (9) and (10). The best proposed model ($ANFIS-PSO-M7$) was compared with the mentioned formulations from literature using prediction performance indices (Table 11) and several visual performance comparisons (Figure 7).

In the two-dimensional scatter plots (Figure 7a,b) the proposed $ANFIS-PSO-M7$ model points

are closer to the 1:1 line and show a more linear pattern (coefficient of determination closer to unity) compared to Etemad-Shahidi et al. (2011)'s and Sharafati et al. (2018)'s models for both live-bed and clear-water scour conditions. The better performance of the $ANFIS-PSO-M7$ model is also confirmed by the heat maps (Figure 7c,d) and the Taylor diagrams (Figure 7e,f).

Although the ANFIS-PSO model provides a better prediction performance compared to the formulas obtained by Etemad-Shahidi et al. (2011) and Sharafati et al. (2018), its additional structure complexity may potentially hinder its application by some practitioners in the field of scouring. Indeed, the ANFIS model comprises several unknown parameters which needs tuning with an optimization algorithm such as PSO. Hence, we especially advise to use the model proposed in the present study in high-stakes pipeline projects that require a very accurate prediction of scour depth.

[Table 11]

[Fig. 7]

To verify that the best predictive model (ANFIS-PSO-M7) is consistent with the physics of the pipeline scour phenomenon, Figure 8 shows how the normalized scour depth *S*/*D* is predicted to vary with varying *e*/*D*, θ, and *KC* in live-bed conditions. The ANFIS-PSO-M7 correctly predicts *S*/*D* to increase for decreasing *e*/*D* or increasing θ and *KC*, as observed in physical investigations (Sumer and Fredsøe 2002).

[Fig. 8]

7.3. Uncertainty analysis of the proposed predictive models

The uncertainty associated with the model structure is evaluated considering the considered five

models ($ANFIS, ANFIS-PSO, ANFIS-ACO, ANFIS-DE$ and $ANFIS-GA$) with $M7$ input variable combination (the best performing combination as shown earlier). The uncertainty associated with the input variables is assessed for the $ANFIS-PSO$ model (the best performing model, as explained earlier) and different input variable combinations ($M1$ to $M7$). Figures 9 and 10 show the generated 95 PPU band, for model structure and input variable uncertainty, respectively. The figures also show the corresponding observed values and are provided for both live-bed and clear-water scour conditions.

From Figure 9, the uncertainty in predicted scour depth associated with the model structure in clear-water ($R-factor=2.53$) is higher than in live-bed conditions ($R-factor=1.87$). From Figure 10, the uncertainty in predicted scour depth associated with the input variables is also higher in clear water ($R-factor=5.11$) compared with live-bed conditions ($R-factor=3.44$). It can generally be concluded that prediction of scour depth caused by waves at pipelines in clear-water conditions is characterized by more considerable uncertainty, due to both model structure and input variables, than in live-bed conditions. Furthermore, the uncertainty associated with the input variables $\left(R-factor_{ave}=\frac{(5.11+3.44)}{2}=4.3\right)$ is larger than the one associated with the model structure $\left(R-factor_{ave}=\frac{(2.53+1.87)}{2}=2.2\right)$.

[Fig. 9]

[Fig. 10]

8. Summary and Conclusion

This study proposed and assessed the application of nature-inspired optimization algorithms to enhance the ANFIS model performance in predicting wave-induced pipeline scour depth. The

considered algorithms (PSO, ACO, DE & GA) are alternatives to the common trial and error methods for optimization, which are not time-efficient and may lead to overfitting.

The proposed models were trained and tested using four datasets (Lucassen 1984; Sumer and Fredsøe 1990; Pu et al. 2001; Mousavi et al. 2009), considering different combinations of input variables (e/D , θ and KC) derived from dimensional analysis. The prediction accuracy of the various proposed models was assessed based on indices of prediction performance (RMSE, MAE, R^2, WI) and visual comparison (heatmap of standardized performance metrics, scatter plot, normalized Taylor diagram and boxplot of the predicted and observed scour depth). From the comparison results, it emerged that the ANFIS model including all the three input variables and optimized using a PSO algorithm provides the most accurate wave-induced pipeline scour depth predictions, for both live-bed and clear-water scour conditions.

This paper also evaluated two sources of uncertainty associated with the scour depth prediction, disaggregating the uncertainty of the model structure (type of optimization algorithm) and the one due to the input variable combination (selection of input variables for the model). To evaluate uncertainty, a Monte Carlo simulation technique is used, and the 95 percent prediction uncertainty is quantified through the $R-factor$ index. From the results, the model structure and the input parameter selection both lead to more considerable uncertainty in scour depth prediction for clear-water conditions than for live-bed conditions. Also, the uncertainty due to the input variable combination is larger than the model structure-associated uncertainty.

This study shows that a relatively simple improvement in the optimization of an ANFIS model, based on the PSO algorithm, may lead to significant improvement in prediction performance not only in comparison with a classic ANFIS model optimized through trial and error procedure, but also in comparison with recently developed models based on the MT approach (Etemad-Shahidi

et al. 2011) or GLUE and SUFI stochastic approaches (Sharafati et al. 2018). The added complexity of the ANFIS-PSO model compared to simpler formulations (still suitable for most projects) is counterbalanced by a higher accuracy.

This paper provides new insight into scouring depth prediction for the design of submarine pipelines. Although the use of conventional equations is straightforward for practical purposes, their prediction is not always accurate. This study shows that an ANFIS-PSO model can be trained and applied for more accurate scour depth predictions that can support a more robust and safer design.

Conflict of interest: Author declare no conflict of interest.

References

Afshar A, Massoumi F, Afshar A, Mariño MA (2015) State of the Art Review of Ant Colony Optimization Applications in Water Resource Management. Water Resour. Manag. 29:3891–3904

Ajay Adithyan T, Sharma V, Gururaj B, Thirumalai C (2018) Nature inspired algorithm. In: Proceedings - International Conference on Trends in Electronics and Informatics, ICEI 2017. pp 1131–1134

Akib S, Mohammadhassani M, Jahangirzadeh A (2014) Application of ANFIS and LR in prediction of scour depth in bridges. Comput Fluids 91:77–86. doi: 10.1016/j.compfluid.2013.12.004

Azamathulla HM, Ghani AA (2010) Genetic Programming to Predict River Pipeline Scour. J Pipeline Syst Eng Pract. doi: 10.1061/(ASCE)PS.1949-1204.0000060

Azamathulla HM, Ghani AA (2011) ANFIS-Based Approach for Predicting the Scour Depth at Culvert Outlets. J Pipeline Syst Eng Pract. doi: 10.1061/(ASCE)PS.1949-1204.0000066

Azamathulla HM, Zakaria NA (2011) Prediction of scour below submerged pipeline crossing a river using ANN. Water Sci. Technol.

Blum C (2005) Ant colony optimization: Introduction and recent trends. Phys. Life Rev.

Çevik E, Yüksel Y (1999) Scour under Submarine Pipelines in Waves in Shoaling Conditions. J Waterw Port, Coastal, Ocean Eng 125:9–19. doi: 10.1061/(asce)0733-950x(1999)125:1(9)

Chen XY, Chau KW (2016) A Hybrid Double Feedforward Neural Network for Suspended Sediment Load Estimation. Water Resour Manag 30:2179–2194. doi: 10.1007/s11269-016-1281-2

Choi SU, Choi B, Lee S (2017) Prediction of local scour around bridge piers using the ANFIS method. Neural Comput Appl. doi: 10.1007/s00521-015-2062-1

Deb K, Pratap A, Agarwal S, Meyarivan T (2002) A fast and elitist multiobjective genetic algorithm: NSGA-II. IEEE Trans Evol Comput 6:182–197. doi: 10.1109/4235.996017

Dorigo M, Blum C (2005) Ant colony optimization theory: A survey. Theor Comput Sci. doi: 10.1016/j.tcs.2005.05.020
Dorigo M, Di Caro G (1999) Ant colony optimization: A new meta-heuristic. In: Proceedings of the 1999 Congress on Evolutionary Computation, CEC 1999
Dorigo M, Maniezzo V, Colorni A (1996) Ant system: Optimization by a colony of cooperating agents. IEEE Trans Syst Man, Cybern Part B Cybern. doi: 10.1109/3477.484436
Dorigo M, Socha K (2007) Ant colony optimization. In: Handbook of Approximation Algorithms and Metaheuristics
Eberhart R, Kennedy J (1995) A new optimizer using particle swarm theory. MHS'95. Proc. Sixth Int. Symp. Micro Mach. Hum. Sci. 39–43
Ebtehaj I, Bonakdari H, Moradi F, et al (2018) An integrated framework of Extreme Learning Machines for predicting scour at pile groups in clear water condition. Coast Eng. doi: 10.1016/j.coastaleng.2017.12.012
Etemad-Shahidi A, Yasa R, Kazeminezhad MH (2011) Prediction of wave-induced scour depth under submarine pipelines using machine learning approach. Appl Ocean Res 33:54–59
Fredsøe J, Hansen EA, Mao Y, Sumer BM (1988) Three-Dimensional Scour Below Pipelines. J Offshore Mech Arct Eng 110:373–379. doi: 10.1115/1.3257075
Ghorbani MA, Deo RC, Yaseen ZM, Kashani MH (2017) Pan evaporation prediction using a hybrid multilayer perceptron-firefly algorithm (MLP-FFA) model : case study in North Iran. doi: 10.1007/s00704-017-2244-0
Guo P, Zhu L (2012) Ant colony optimization for continuous domains. In: Proceedings - International Conference on Natural Computation
Haghiabi AH (2017) Prediction of river pipeline scour depth using multivariate adaptive regression splines. J Pipeline Syst Eng Pract. doi: 10.1061/(ASCE)PS.1949-1204.0000248
Haghiabi AH (2019) Closure to "prediction of River Pipeline Scour Depth Using Multivariate Adaptive Regression Splines" by Amir Hamzeh Haghiabi. J. Pipeline Syst. Eng. Pract.
Hai T, Sharafati A, Mohammed A, et al (2020) Global solar radiation estimation and climatic variability analysis using extreme learning machine based predictive model. IEEE Access 8:12026–12042
Homaei F, Najafzadeh M (2020) A reliability-based probabilistic evaluation of the wave-induced scour depth around marine structure piles. Ocean Eng 196:106818
Iba H, Aranha CC (2012) Introduction to genetic algorithms. Adapt. Learn. Optim.
Jang J-S (1996) Input selection for ANFIS learning. In: Fuzzy Systems, 1996., Proceedings of the Fifth IEEE International Conference on. pp 1493–1499
Kazeminezhad MH, Etemad-Shahidi a., Yeganeh Bakhtiary a. (2010) An alternative approach for investigation of the wave-induced scour around pipelines. J Hydroinformatics. doi: 10.2166/hydro.2010.042
Khalid M, Muzzammil M, Alam J (2019) A reliability-based assessment of live bed scour at bridge piers. ISH J Hydraul Eng 1–8
Kisi O, Yaseen ZM (2019) The potential of hybrid evolutionary fuzzy intelligence model for suspended sediment concentration prediction. Catena 174:11–23. doi: 10.1016/j.catena.2018.10.047
Koza JR (1994) Genetic programming as a means for programming computers by natural selection. Stat Comput 4:87–112
Kubat M (2017) The Genetic Algorithm. In: An Introduction to Machine Learning
Levasseur S, Malécot Y, Boulon M, Flavigny E (2008) Soil parameter identification using a

genetic algorithm. Int J Numer Anal Methods Geomech. doi: 10.1002/nag.614
Li Y, Chan Hilton AB (2005) Reducing spatial sampling in long-term groundwater monitoring networks using ant colony optimization. Int J Comput Intell Res 1:19–28. doi: 10.5019/ijcir.2005.1.2
Li Y, Chan Hilton AB (2007) Optimal groundwater monitoring design using an ant colony optimization paradigm. Environ Model Softw 22:110–116. doi: 10.1016/j.envsoft.2006.05.023
Lucassen RJ (1984) Scour underneath submarine pipelines
Maier HR, Kapelan Z, Kasprzyk J, et al (2014) Evolutionary algorithms and other metaheuristics in water resources: Current status, research challenges and future directions. Environ Model Softw 62:271–299. doi: 10.1016/j.envsoft.2014.09.013
Malik A, Kumar A, Kim S, et al (2020) Modeling monthly pan evaporation process over the Indian central Himalayas: application of multiple learning artificial intelligence model. Eng Appl Comput Fluid Mech 14:323–338
Maulik U, Bandyopadhyay S (2000) Genetic algorithm-based clustering technique. Pattern Recognit 33:1455–1465. doi: 10.1016/S0031-3203(99)00137-5
Mohammed M, Sharafati A, Al-Ansari N, Yaseen ZM (2020) Shallow Foundation Settlement Quantification: Application of Hybridized Adaptive Neuro-Fuzzy Inference System Model. Adv Civ Eng 2020:
Moradi F, Bonakdari H, Kisi O, et al (2018) Abutment scour depth modeling using neuro-fuzzy-embedded techniques. Mar Georesources Geotechnol. doi: 10.1080/1064119X.2017.1420113
Motahari M, Mazandaranizadeh H (2017) Development of a PSO-ANN Model for Rainfall-Runoff Response in Basins, Case Study: Karaj Basin. Civ Eng J 3:35–44
Mousavi ME, Bakhtiary AY, Enshaei N (2009) The Equivalent Depth of Wave-Induced Scour Around Offshore Pipelines. J Offshore Mech Arct Eng Asme. doi: Artn 021601\rDoi 10.1115/1.3058681
Najafzadeh M (2015) Neuro-fuzzy GMDH based particle swarm optimization for prediction of scour depth at downstream of grade control structures. Eng Sci Technol an Int J 18:42–51. doi: 10.1016/j.jestch.2014.09.002
Najafzadeh M, Barani G-A, Hessami Kermani MR (2014a) Estimation of Pipeline Scour due to Waves by GMDH. J Pipeline Syst Eng Pract 5:. doi: 10.1061/(asce)ps.1949-1204.0000171
Najafzadeh M, Barani GA, Azamathulla HM (2014b) Prediction of pipeline scour depth in clear-water and live-bed conditions using group method of data handling. Neural Comput Appl 24:629–635. doi: 10.1007/s00521-012-1258-x
Najafzadeh M, Etemad-Shahidi A, Lim SY (2016) Scour prediction in long contractions using ANFIS and SVM. Ocean Eng. doi: 10.1016/j.oceaneng.2015.10.053
Najafzadeh M, Kargar AR (2019) Gene-expression programming, evolutionary polynomial regression, and model tree to evaluate local scour depth at culvert outlets. J Pipeline Syst Eng Pract 10:04019013. doi: 10.1061/(ASCE)PS.1949-1204.0000376
Najafzadeh M, Rezaie-Balf M, Tafarojnoruz A (2018) Prediction of riprap stone size under overtopping flow using data-driven models. Int J River Basin Manag. doi: 10.1080/15715124.2018.1437738
Najafzadeh M, Saberi-Movahed F (2018) GMDH-GEP to predict free span expansion rates below pipelines under waves. Mar. Georesources Geotechnol.
Najafzadeh M, Sarkamaryan S (2018) Extraction of optimal equations for evaluation of pipeline

scour depth due to currents. Proc Inst Civ Eng - Marit Eng. doi: 10.1680/jmaen.2017.10
Najafzadeh M, Tafarojnoruz A (2016) Evaluation of neuro-fuzzy GMDH-based particle swarm optimization to predict longitudinal dispersion coefficient in rivers. Environ Earth Sci 75:. doi: 10.1007/s12665-015-4877-6
Najafzadeh M, Tafarojnoruz A, Lim SY (2017) Prediction of local scour depth downstream of sluice gates using data-driven models. ISH J Hydraul Eng 23:195–202. doi: 10.1080/09715010.2017.1286614
Parsaie A, Haghiabi AH, Moradinejad A (2019) Prediction of Scour Depth below River Pipeline using Support Vector Machine. KSCE J Civ Eng. doi: 10.1007/s12205-019-1327-0
Pu Q, Li K, Gao F (2001) Scour of the seabed under a pipeline in oscillating flow. China Ocean Eng 15:129–138
Salamatian SA, Zarrati AR (2019) Reliability study on uncertainty parameters and flood duration on scouring around unprotected and protected bridge piers. ISH J Hydraul Eng 1–9
Salih SQ, Sharafati A, Ebtehaj I, et al (2020) Integrative stochastic model standardization with genetic algorithm for rainfall pattern forecasting in tropical and semi-arid environments. Hydrol Sci J 1–13
Salih SQ, sharafati A, Khosravi K, et al (2019) River suspended sediment load prediction based on river discharge information: application of newly developed data mining models. Hydrol Sci J
Sharafati A, Asadollah SBHS, Hosseinzadeh M (2020a) The potential of new ensemble machine learning models for effluent quality parameters prediction and related uncertainty. Process Saf Environ Prot
Sharafati A, Azamathulla HM (2018) Assessment of Dam Overtopping Reliability using SUFI Based Overtopping Threshold Curve. Water Resour Manag 32:2369–2383
Sharafati A, Haghbin M, Motta D, Yaseen ZM (2019) The Application of Soft Computing Models and Empirical Formulations for Hydraulic Structure Scouring Depth Simulation: A Comprehensive Review, Assessment and Possible Future Research Direction. Arch Comput Methods Eng 1–25
Sharafati A, Tafarojnoruz A, Yaseen ZM (2020b) New stochastic modeling strategy on the prediction enhancement of pier scour depth in cohesive bed materials. J Hydroinformatics
Sharafati A, Yasa R, Azamathulla HM (2018) Assessment of Stochastic Approaches in Prediction of Wave-Induced Pipeline Scour Depth. J Pipeline Syst Eng Pract 9:4018024
Sharafati A, Zahabiyoun B (2014) Rainfall Threshold Curves Extraction by Considering Rainfall-Runoff Model Uncertainty. Arab J Sci Eng 39:. doi: 10.1007/s13369-014-1246-9
Storn R, Price K (1995) Differential evolution-a simple and efficient adaptive scheme for global optimization over continuous spaces. Int. Comput. Sci. Institute-Publications-Tr 1–12
Sumer BM, Fredsøe J (1990) Scour below Pipelines in Waves. J Waterw Port, Coastal, Ocean Eng. doi: 10.1061/(ASCE)0733-950X(1990)116:3(307)
Sumer BM, Fredsøe J (2002) The Mechanics of Scour in the Marine Environment. World Scientific, Singapore
Surco DF, Vecchi TPB, Ravagnani MASS (2018) Optimization of water distribution networks using a modified particle swarm optimization algorithm. Water Sci Technol Water Supply 18:660–678. doi: 10.2166/ws.2017.148
Suribabu CR (2010) Differential evolution algorithm for optimal design of water distribution networks. J Hydroinformatics. doi: 10.2166/hydro.2010.014
Tafarojnoruz A (2012) Discussion of “Genetic programming to predict bridge pier scour.” J

Hydraul Eng 138:669–671. doi: 10.1061/(ASCE)HY.1943-7900.0000388
Tafarojnoruz A, Gaudio R (2012) Discussion on “Scale effects in physical hydraulic engineering models.” J Hydraul Res 50:247–248. doi: 10.1080/00221686.2012.668377
Taylor KE (2001) Summarizing multiple aspects of model performance in a single diagram. J Geophys Res Atmos 106:7183–7192. doi: 10.1029/2000JD900719
Weise T (2009) Global Optimization Algorithms–Theory and Application. Self-Published 1:820. doi: doi=10.1.1.64.8184
Wu Z, Luo Z (2020) Life-Cycle System Reliability-Based Approach for Bridge Pile Foundations under Scour Conditions. KSCE J Civ Eng 1–12
Yang J, Honavar V (1998) Feature subset selection using genetic algorithm. IEEE Intell Syst Their Appl. doi: 10.1109/5254.671091
Yasa R, Etemad-Shahidi A (2014) Classification and regression trees approach for predicting current-induced scour depth under pipelines. J Offshore Mech Arct Eng 136:011702. doi: 10.1115/1.4025654
Yaseen ZM, Ebtehaj I, Bonakdari H, et al (2017) Novel approach for streamflow forecasting using a hybrid ANFIS-FFA model. J Hydrol
Yaseen ZM, El-shafie A, Jaafar O, et al (2015) Artificial intelligence based models for stream-flow forecasting: 2000–2015. J Hydrol 530:829–844. doi: 10.1016/j.jhydrol.2015.10.038
Zadeh L (1965) Fuzzy Sets. Inf. Control 8:338–353
Zanganeh M, Yeganeh-Bakhtiary A, Bakhtyar R (2011) Combined particle swarm optimization and fuzzy inference system model for estimation of current-induced scour beneath marine pipelines. J HYDROINFORMATICS. doi: 10.2166/hydro.2010.101
Zhao E, Shi B, Qu K, et al (2018) Experimental and Numerical Investigation of Local Scour Around Submarine Piggyback Pipeline Under Steady Current. J Ocean Univ China 17:244–256. doi: 10.1007/s11802-018-3290-7
Zhao Z, Fernando HJS (2007) Numerical simulation of scour around pipelines using an Euler–Euler coupled two-phase model. Environ Fluid Mech 7:121–142. doi: 10.1007/s10652-007-9017-8

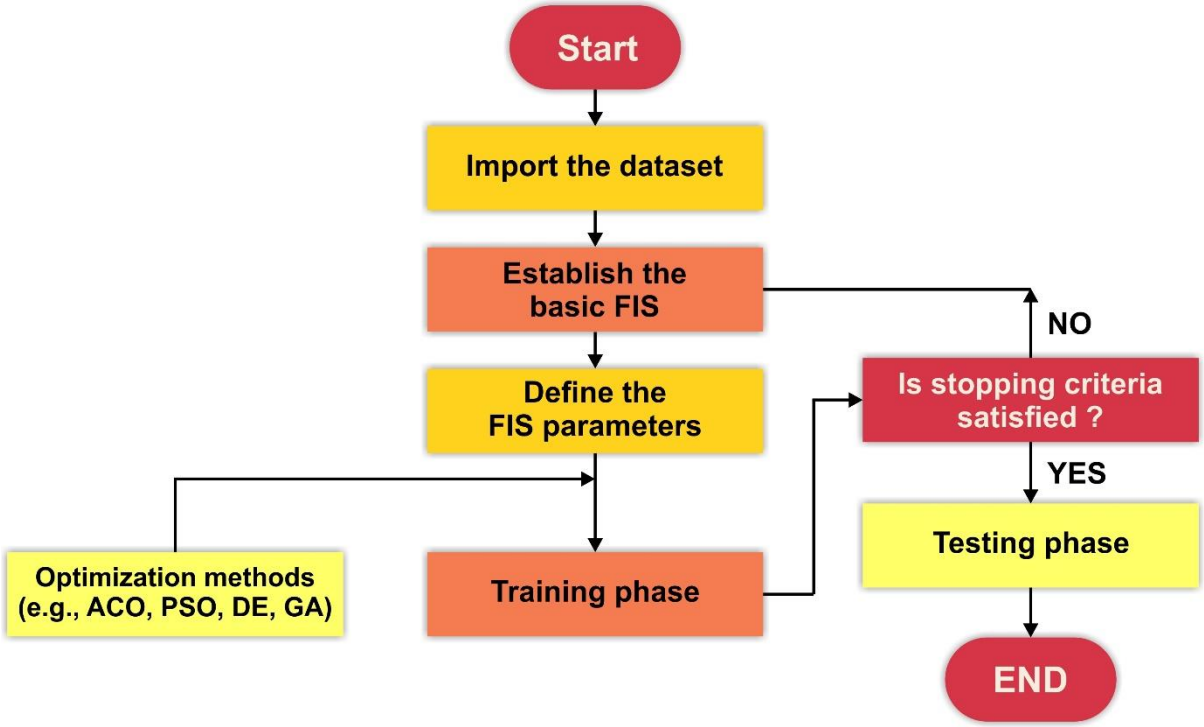

Figure 1. Proposed integrated ANFIS models with nature-inspired optimization algorithms (PSO, ACO, DE and GA)

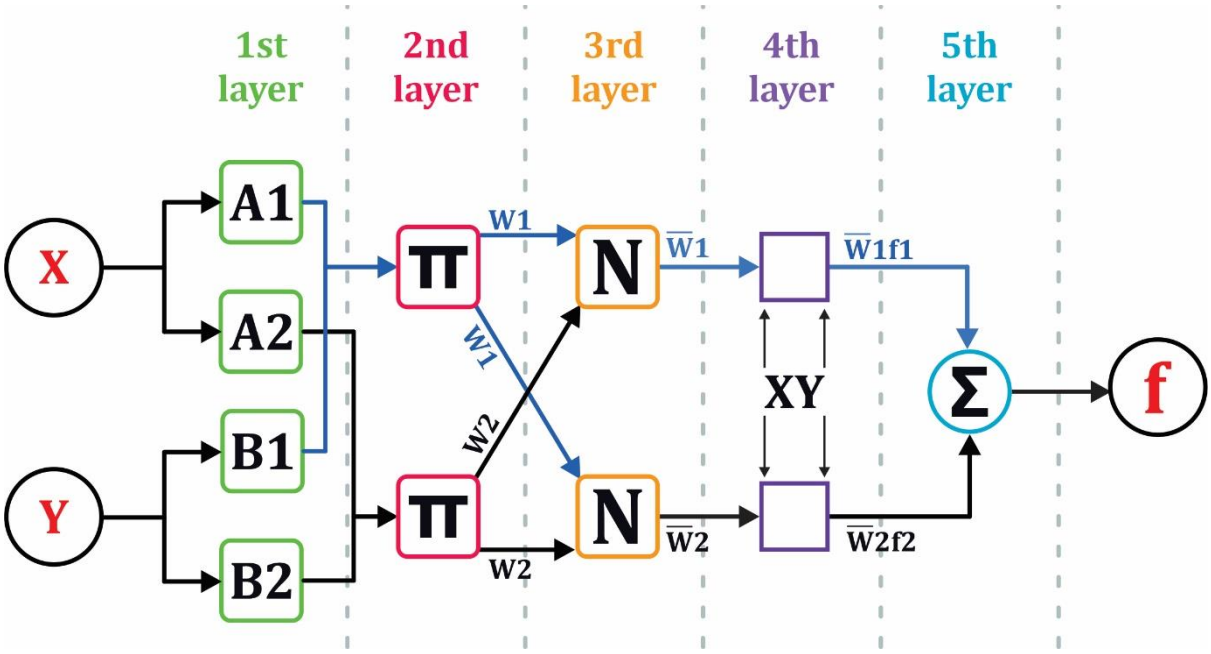

Figure 2. Conceptual structure of an ANFIS model

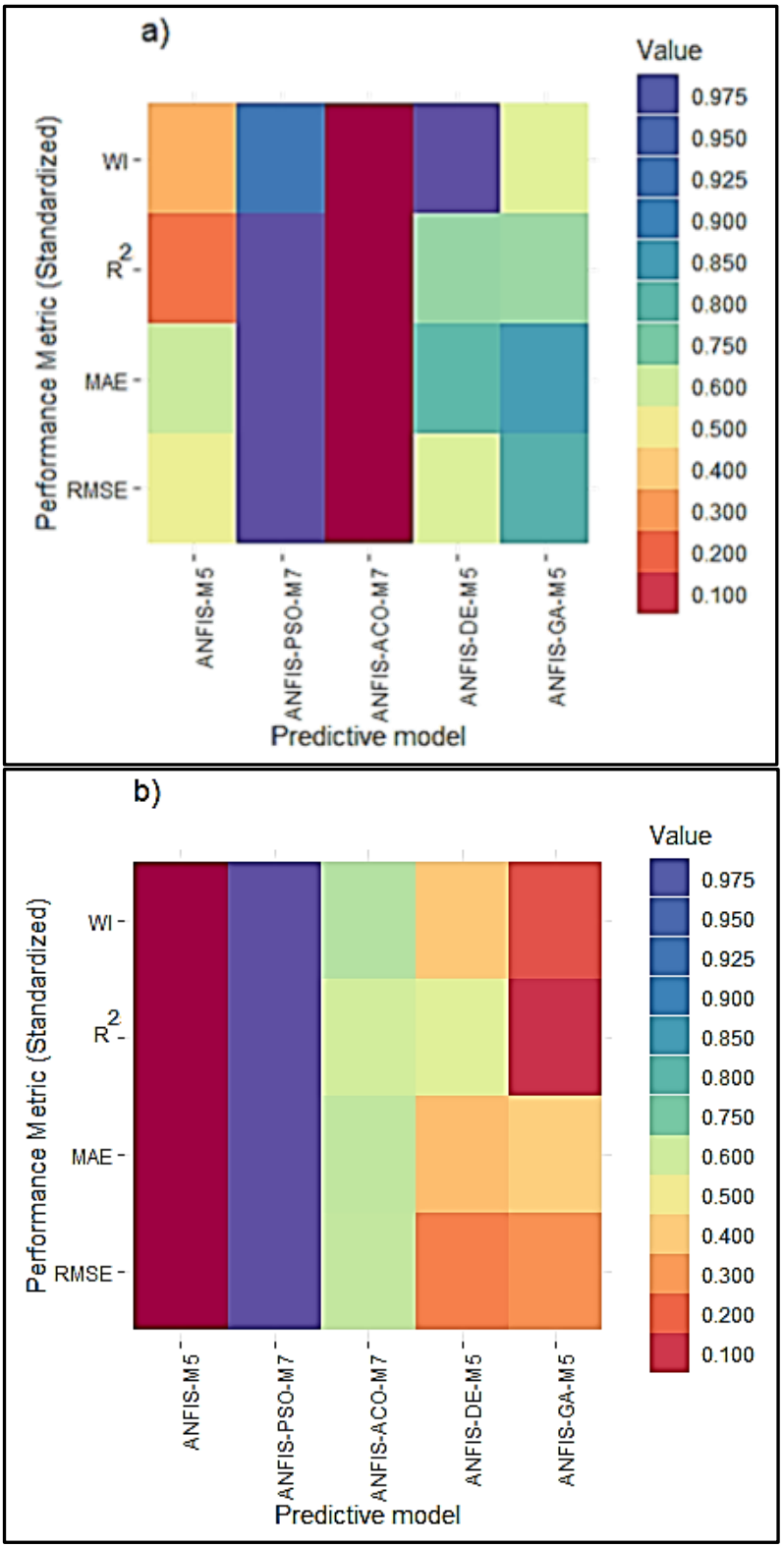

Figure 3. Heat map of scour depth model prediction performance, based on four standardized performance metrics, for testing phase in (a) live-bed and (b) clear-water conditions

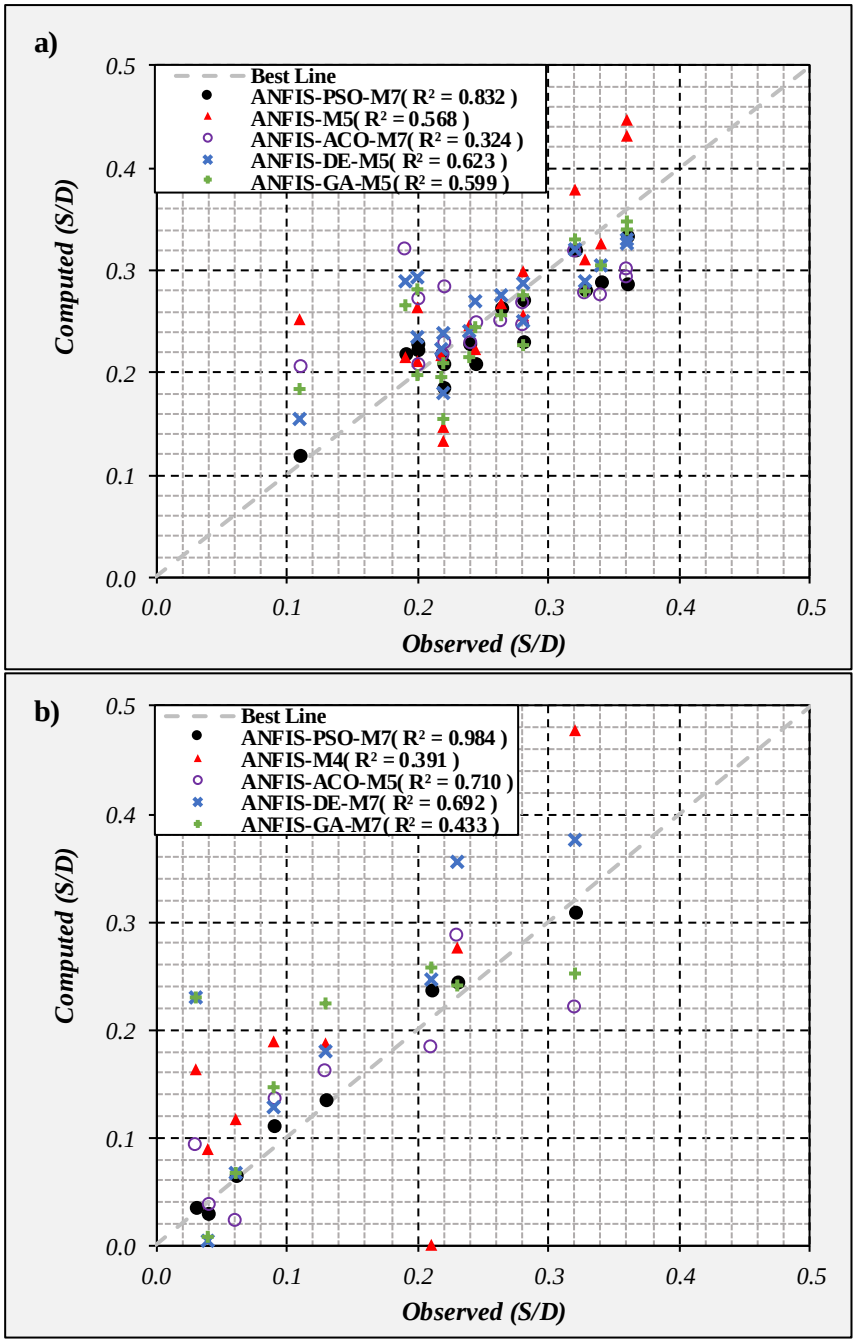

Figure 4. Scatter plot of computed vs. observed scour depth in testing phase for (a) live-bed and (b) clear-water conditions

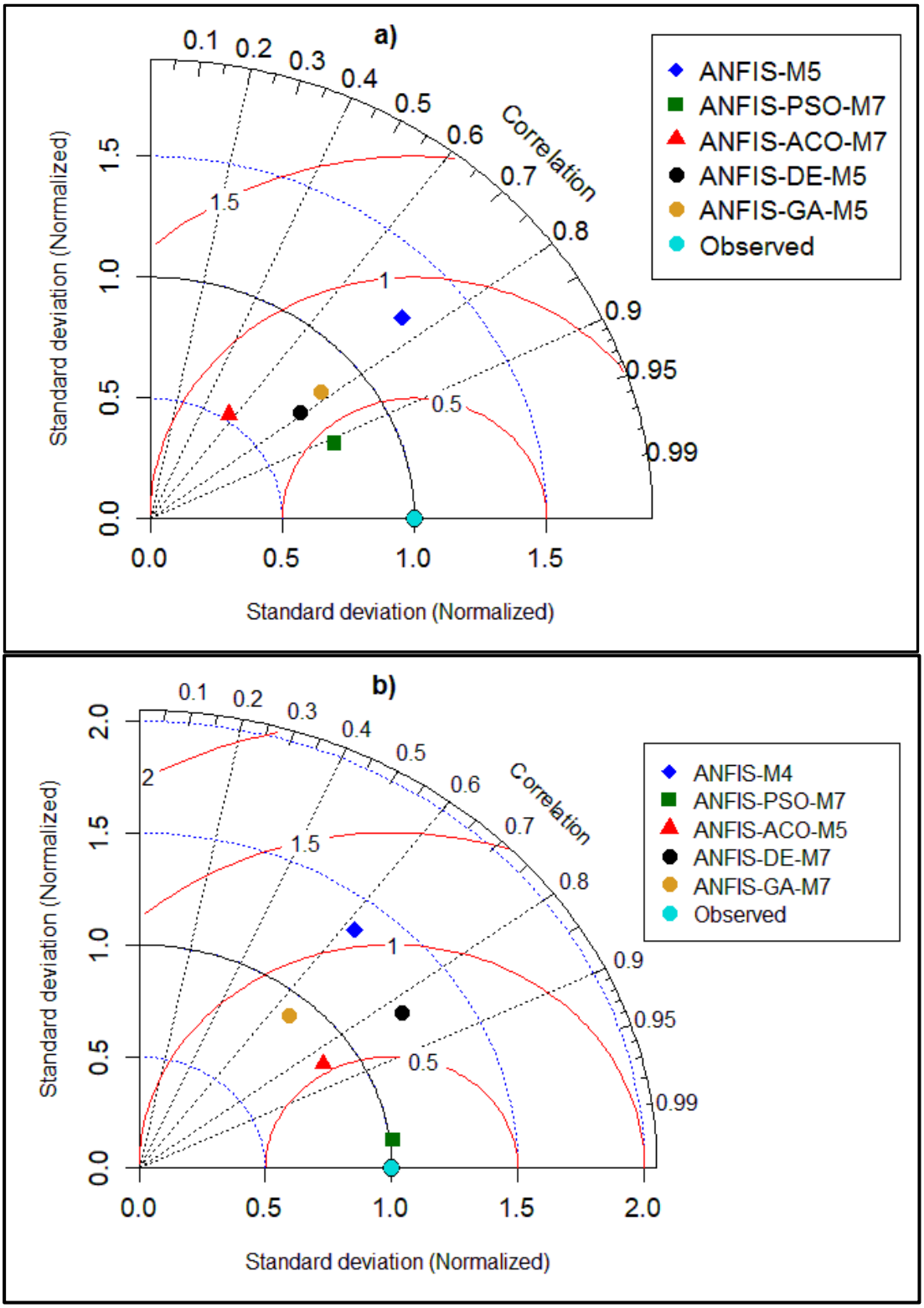

Figure 5. Normalized Taylor diagrams of the predicted and the observed scour depth in testing phase for (a) live-bed conditions (b) clear-water conditions

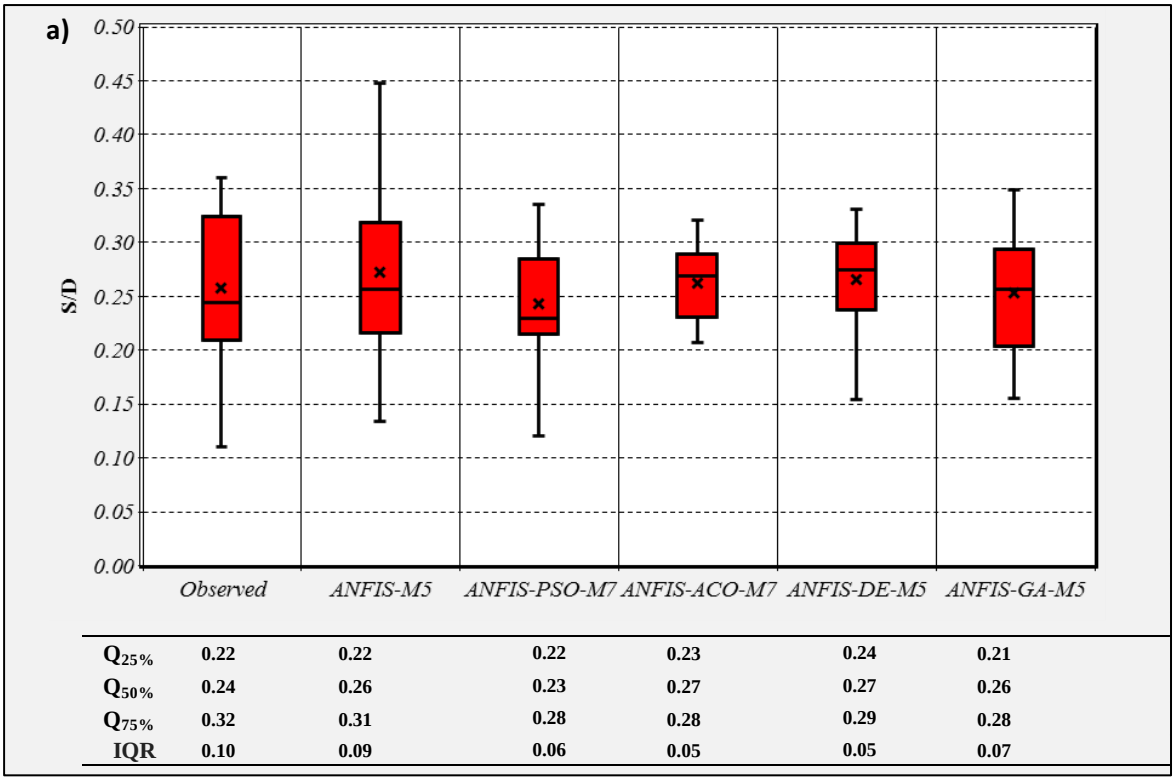

$Q_{25\%}$	0.22	0.22	0.22	0.23	0.24	0.21
$Q_{50\%}$	0.24	0.26	0.23	0.27	0.27	0.26
$Q_{75\%}$	0.32	0.31	0.28	0.28	0.29	0.28
IQR	0.10	0.09	0.06	0.05	0.05	0.07

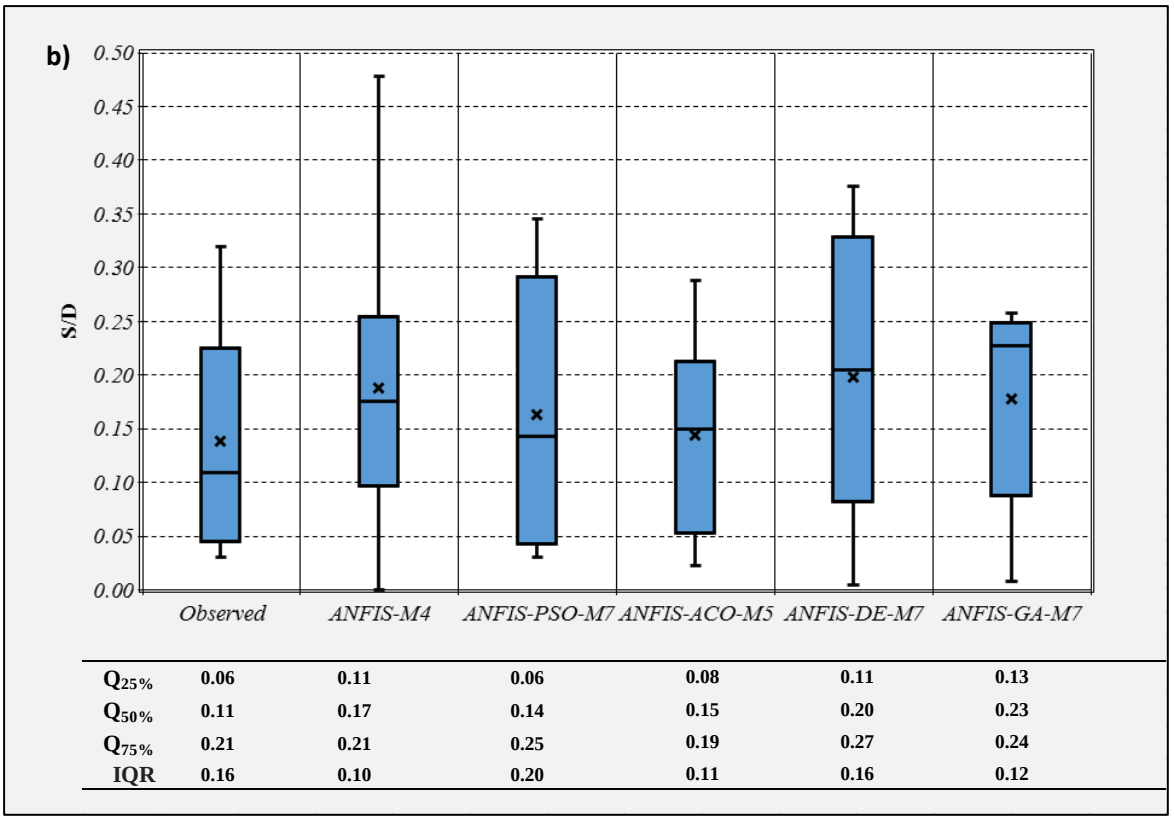

$Q_{25\%}$	0.06	0.11	0.06	0.08	0.11	0.13
$Q_{50\%}$	0.11	0.17	0.14	0.15	0.20	0.23
$Q_{75\%}$	0.21	0.21	0.25	0.19	0.27	0.24
IQR	0.16	0.10	0.20	0.11	0.16	0.12

Figure 6. Boxplot of observed and predicted scour depth in testing phase for (a) live-bed and (b) clear-water conditions

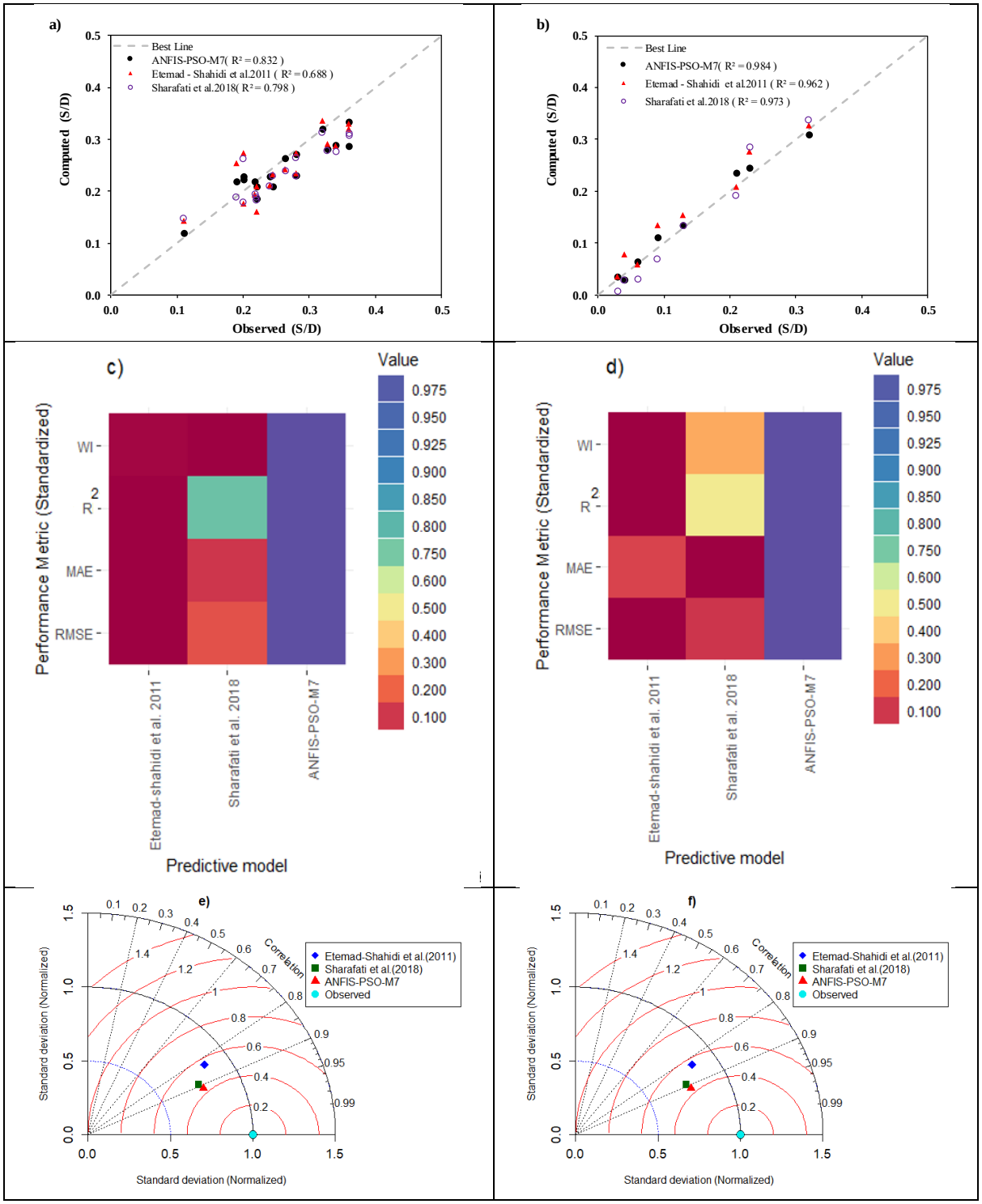

Figure 7. Comparison between the best proposed predictive model (ANFIS-PSO-M7) from this study and recently developed models for testing phase. a) Scatter plot for live-bed conditions, b) Scatter plot for clear-water conditions, c) Heat map of standardized performance metrics for live bed conditions, d) Heat map of standardized performance metrics for clear-water conditions, e) Taylor diagram for live-bed conditions, f) Taylor diagram for clear-water conditions

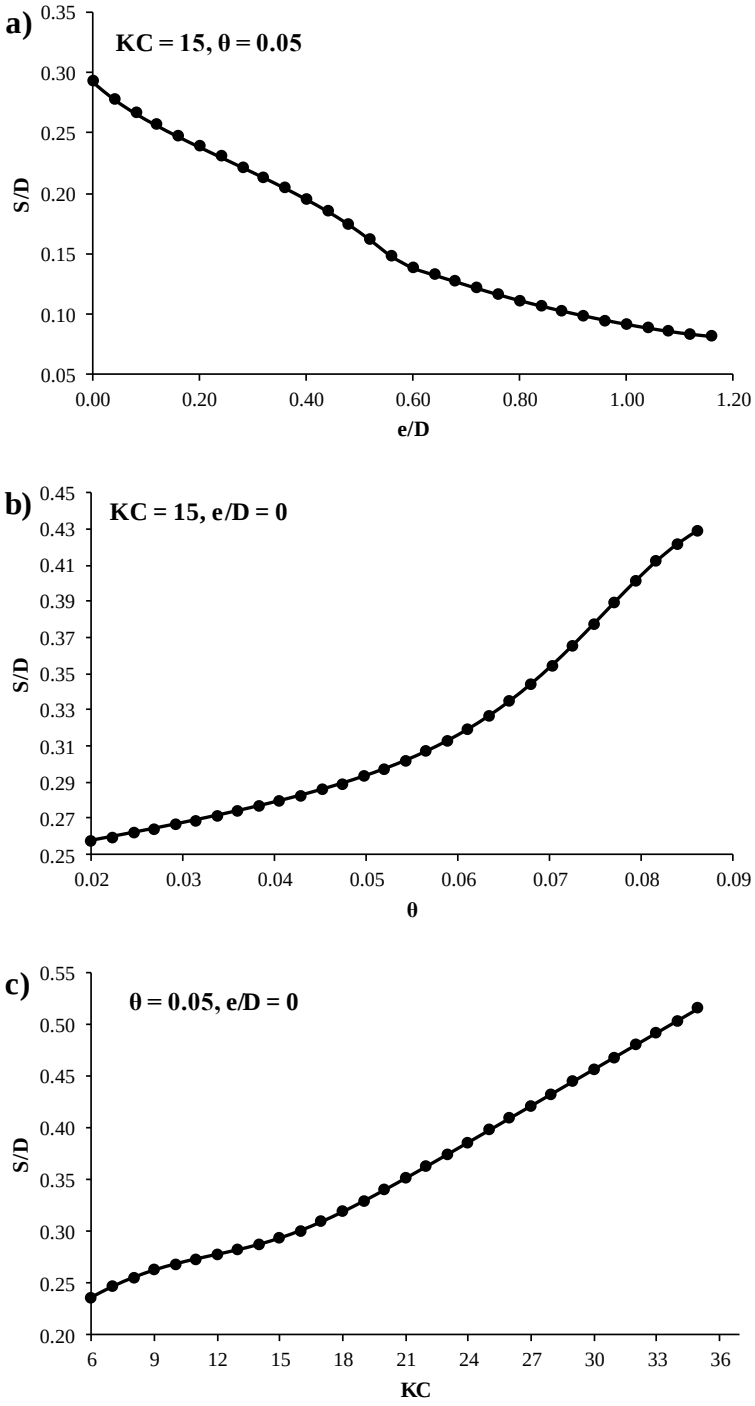

Figure 8. Normalized scour depth in live-bed as function of a) normalized distance between pipeline and sea bed, b) Shields number and c) Keulegan–Carpenter number

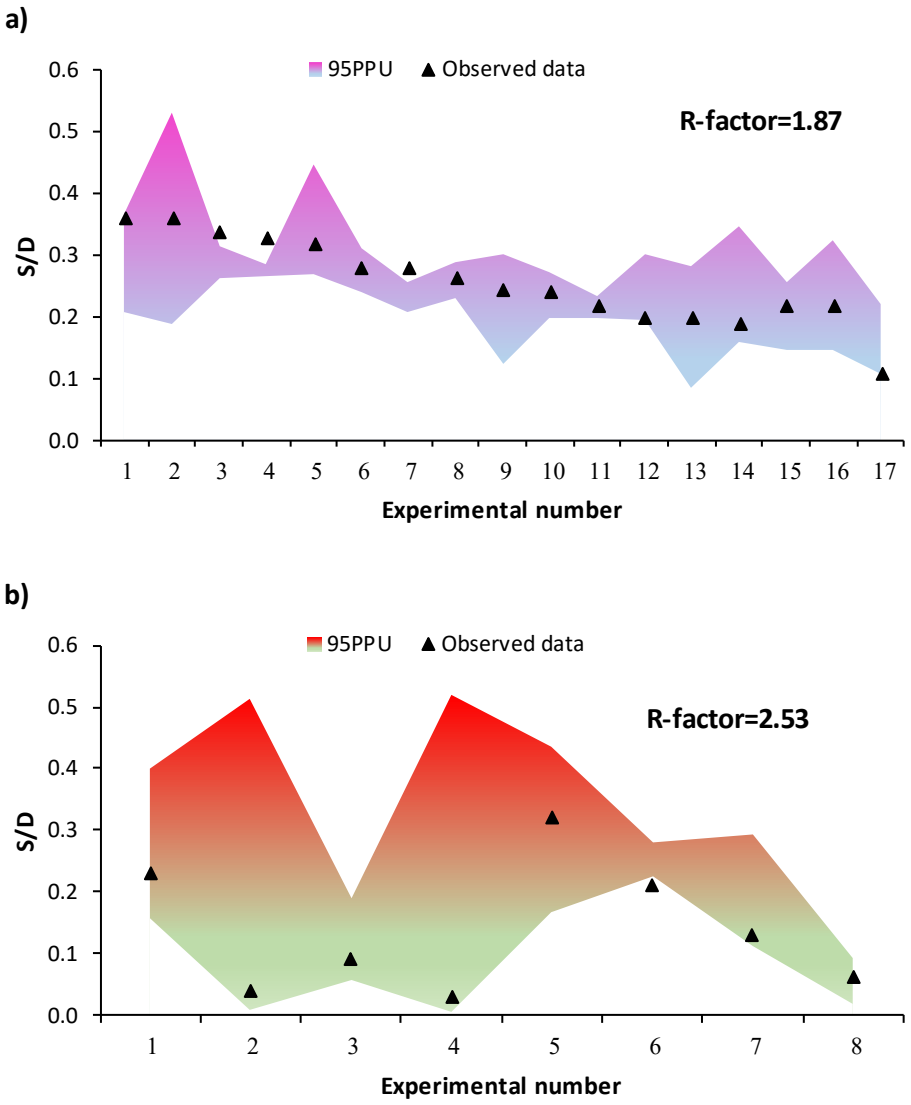

Figure 9. Generated 95 PPU band accounting for model structure uncertainty for (a) live-bed and (b) clear-water conditions

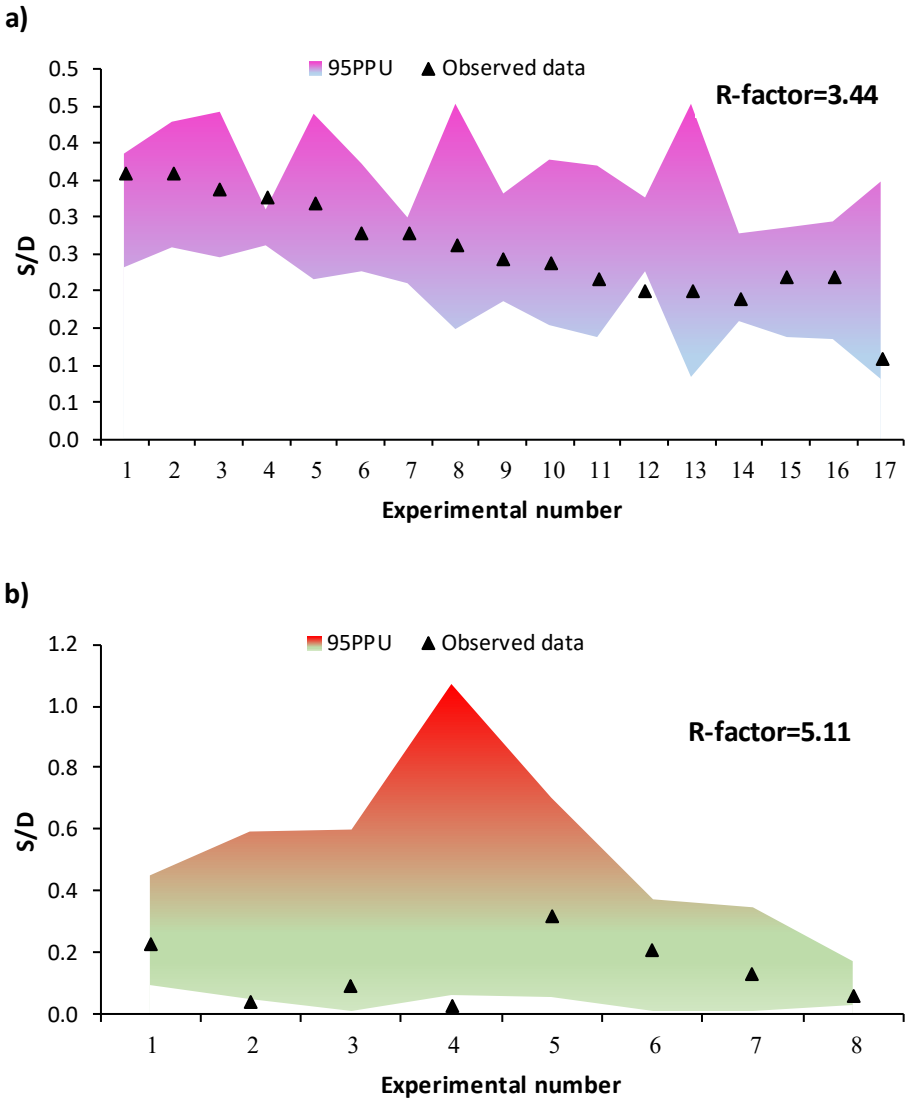

Figure 10. Generated 95 PPU band accounting for the input variable combination uncertainty for (a) live-bed and (b) clear-water conditions

Table 1. Parameters used for application of the various optimization techniques

Optimization technique	Description of the parameter	Parameter value
PSO	Number of Iterations	1500
	Number of Populations	50
	Inertia Weight	1
	Inertia Weight Damping Ratio	0.99
	Personal Learning Coefficient	0.9
	Global Learning Coefficient	2
ACO	Number of Iterations	1500
	Number of Populations	50
	Intensification Factor	0.5
	Deviation-Distance Ratio	1
DE	Lower Bound of Scaling Factor	0.2
	Upper Bound of Scaling Factor	0.8
	Crossover Probability	0.15
GA	Number of Iterations	1500
	Number of Populations	50
	Crossover Percentage	0.7
	Number of Offsprings	80 (Crossover Percentage * Number of Populations)
	Mutation Rate	0.15
	Mutation Percentage	0.45
	Number of Mutants	60 (Mutation Percentage * Number of Populations)
	Selection Pressure	8
ANFIS	Train Epochs	250
	Train-Error Goal	0
	Train-Initial Step Size	0.015
	Train-Step Size Decrease	0.95
	Train-Step Size Increase	1.15

Table 2: Optimized parameters for the ANFIS-PSO model

Model	Condition	Antecedent Parameters							Consequent Parameters				
		Membership function	KC		θ		e/D		Membership function	p	q	r	s
			a	b	a	b	a	b					
ANFIS-PSO	Live-bed	Gaussian	76.97	10.48	0.026	0.0092	0.101	0.194	Linear	0.012	0.855	-0.179	0.06
			11.02	-29.23	0.069	-0.486	-2.18	0.28		0.032	-0.025	-0.109	-0.229
	Clear-water		1.65	11.73	0.039	0.12	-0.77	0.35		0.011	-2.08	1.16	-0.19

Table 3. Combinations of input variables to predict wave-induced scour depth at pipelines

Input Combination	Predictive Variables		
	KC	θ	e/D
M1	✓		
M2		✓	
M3			✓
M4	✓	✓	
M5	✓		✓
M6		✓	✓
M7	✓	✓	✓

Table 4. Statistical characteristics of dimensionless parameters for the four selected datasets

Parameter	**Inputs**			**Output**
	KC	θ	e/D	S/D
Minimum	1.42	0.02	0.00	0.03
Maximum	55.77	0.28	2.04	0.95
Average	13.40	0.09	0.19	0.26
Standard Deviation	9.97	0.05	0.38	0.16
Coefficient of Variation	0.74	0.58	2.04	0.62

Table 5. Performance indices of the classic ANFIS model for both live-bed and clear-water conditions

Hydraulic Condition	Phase	Input Combination	RMSE	MAE	R^2	WI
Live bed	Training	M1	0.072	0.048	0.623	0.876
		M2	0.099	0.073	0.280	0.640
		M3	0.085	0.068	0.469	0.791
		M4	0.060	0.041	0.738	0.919
		M5	**0.025**	**0.018**	**0.955**	**0.988**
		M6	0.075	0.053	0.589	0.855
		M7	0.028	0.021	0.941	0.985
	Testing	M1	0.077	0.054	0.043	0.552
		M2	0.134	0.103	0.015	0.337
		M3	0.082	0.064	0.275	0.672
		M4	0.049	0.034	0.466	0.794
		M5	**0.058**	**0.043**	**0.568**	**0.837**
		M6	0.073	0.055	0.334	0.717
		M7	0.077	0.061	0.478	0.775
Clear water	Training	M1	0.042	0.028	0.978	0.994
		M2	0.105	0.065	0.858	0.960
		M3	0.268	0.205	0.079	0.332
		M4	**0.013**	**0.010**	**0.998**	**0.999**
		M5	0.039	0.027	0.981	0.995
		M6	0.070	0.053	0.938	0.983
		M7	0.006	0.004	0.997	0.998
	Testing	M1	0.344	0.255	0.010	0.295
		M2	0.516	0.357	0.001	0.171
		M3	0.157	0.128	0.090	0.531
		M4	**0.116**	**0.101**	**0.391**	**0.750**
		M5	0.495	0.359	0.198	0.043
		M6	0.996	0.636	0.364	0.029
		M7	0.245	0.184	0.043	0.269

Table 6. Performance indices of the ANFIS-PSO model for both live-bed and clear-water conditions

Hydraulic Condition	Phase	Input Combination	RMSE	MAE	R^2	WI
Live bed	Training	M1	0.086	0.063	0.457	0.789
		M2	0.099	0.080	0.287	0.665
		M3	0.086	0.070	0.467	0.788
		M4	0.055	0.035	0.779	0.934
		M5	0.031	0.024	0.932	0.982
		M6	0.075	0.053	0.594	0.859
		M7	**0.024**	**0.018**	**0.957**	**0.989**
	Testing	M1	0.075	0.055	0.002	0.448
		M2	0.088	0.070	0.044	0.468
		M3	0.081	0.061	0.286	0.680
		M4	0.047	0.033	0.511	0.787
		M5	0.036	0.029	0.761	0.930
		M6	0.087	0.065	0.250	0.658
		M7	**0.032**	**0.026**	**0.832**	**0.923**
Clear water	Training	M1	0.040	0.029	0.979	0.995
		M2	0.101	0.057	0.933	0.964
		M3	0.268	0.205	0.079	0.332
		M4	0.026	0.018	0.991	0.998
		M5	0.017	0.011	0.996	0.999
		M6	0.076	0.046	0.939	0.978
		M7	**0.0048**	**0.0029**	**0.9997**	**0.9999**
	Testing	M1	0.263	0.219	0.162	0.164
		M2	0.605	0.380	0.131	0.176
		M3	0.222	0.161	0.633	0.634
		M4	0.454	0.383	0.249	0.150
		M5	0.322	0.228	0.360	0.424
		M6	1.533	0.688	0.058	0.031
		M7	**0.014**	**0.012**	**0.984**	**0.995**

Table 7. Performance indices of the ANFIS-ACO model for both live-bed and clear-water conditions

Hydraulic Condition	Phase	Input Combination	RMSE	MAE	R^2	WI
Live bed	Training	M1	0.102	0.072	0.255	0.669
		M2	0.115	0.095	0.032	0.251
		M3	0.102	0.084	0.244	0.607
		M4	0.106	0.088	0.184	0.558
		M5	0.065	0.048	0.697	0.904
		M6	0.101	0.080	0.268	0.565
		M7	0.063	0.049	0.715	0.903
	Testing	M1	0.088	0.069	0.008	0.387
		M2	0.071	0.060	0.162	0.474
		M3	0.070	0.057	0.313	0.665
		M4	0.078	0.062	0.010	0.257
		M5	0.057	0.047	0.288	0.657
		M6	0.066	0.056	0.340	0.675
		M7	**0.055**	**0.041**	**0.324**	**0.692**
Clear water	Training	M1	0.075	0.068	0.929	0.980
		M2	0.204	0.166	0.467	0.804
		M3	0.268	0.205	0.079	0.332
		M4	0.079	0.065	0.919	0.978
		M5	0.076	0.062	0.925	0.980
		M6	0.164	0.122	0.654	0.886
		M7	0.049	0.037	0.970	0.992
	Testing	M1	0.160	0.126	0.124	0.259
		M2	0.348	0.284	0.004	0.333
		M3	0.222	0.161	0.633	0.634
		M4	0.204	0.146	0.031	0.360
		M5	**0.053**	**0.045**	**0.71**	**0.909**
		M6	0.313	0.258	0.849	0.595
		M7	0.116	0.093	0.811	0.837

Table 8. Performance indices of the ANFIS-DE model for both live-bed and clear-water conditions

Hydraulic Condition	Phase	Input Combination	RMSE	MAE	R^2	WI
Live bed	Training	M1	0.097	0.074	0.376	0.726
		M2	0.114	0.092	0.054	0.323
		M3	0.098	0.078	0.311	0.648
		M4	0.099	0.080	0.297	0.701
		M5	0.057	0.042	0.766	0.930
		M6	0.098	0.075	0.331	0.707
		M7	0.060	0.047	0.744	0.915
	Testing	M1	0.081	0.052	0.034	0.549
		M2	0.071	0.059	0.173	0.463
		M3	0.064	0.052	0.372	0.748
		M4	0.077	0.061	0.004	0.284
		M5	**0.042**	**0.032**	**0.623**	**0.863**
		M6	0.063	0.055	0.382	0.755
		M7	0.053	0.042	0.372	0.706
Clear water	Training	M1	0.063	0.053	0.950	0.987
		M2	0.183	0.139	0.600	0.877
		M3	0.268	0.205	0.079	0.332
		M4	0.063	0.054	0.950	0.987
		M5	0.059	0.046	0.958	0.988
		M6	0.155	0.111	0.694	0.907
		M7	0.046	0.037	0.973	0.993
	Testing	M1	0.204	0.164	0.221	0.156
		M2	0.600	0.429	0.002	0.199
		M3	0.222	0.161	0.633	0.634
		M4	0.109	0.086	0.002	0.418
		M5	0.277	0.200	0.069	0.212
		M6	1.745	0.941	0.420	0.121
		M7	**0.090**	**0.068**	**0.692**	**0.846**

Table 9. Performance indices of ANFIS-GA model for both live-bed and clear-water conditions

Hydraulic Condition	Phase	Input Combination	RMSE	MAE	R^2	WI
Live bed	Training	M1	0.085	0.060	0.470	0.796
		M2	0.101	0.079	0.259	0.622
		M3	0.086	0.070	0.465	0.785
		M4	0.072	0.052	0.622	0.875
		M5	0.039	0.027	0.890	0.970
		M6	0.076	0.061	0.578	0.847
		M7	0.041	0.027	0.878	0.967
	Testing	M1	0.072	0.049	0.013	0.477
		M2	0.082	0.070	0.015	0.420
		M3	0.081	0.063	0.280	0.674
		M4	0.066	0.048	0.133	0.575
		M5	**0.042**	**0.032**	**0.599**	**0.870**
		M6	0.065	0.053	0.269	0.683
		M7	0.040	0.034	0.648	0.887
Clear water	Training	M1	0.045	0.035	0.974	0.993
		M2	0.107	0.068	0.853	0.959
		M3	0.268	0.205	0.079	0.332
		M4	0.024	0.017	0.993	0.998
		M5	0.046	0.031	0.973	0.993
		M6	0.095	0.066	0.885	0.968
		M7	0.010	0.007	0.999	0.999
	Testing	M1	0.226	0.191	0.144	0.211
		M2	0.368	0.168	0.034	0.172
		M3	0.222	0.161	0.633	0.634
		M4	0.283	0.234	0.414	0.081
		M5	0.392	0.285	0.630	0.418
		M6	0.557	0.295	0.002	0.185
		M7	**0.087**	**0.065**	**0.433**	**0.789**

Table 10. Best performance indices obtained for each ANFIS model type for the testing phase

Hydraulic Condition	Phase	Model	RMSE	MAE	R^2	WI	IM
Live bed	Testing	ANFIS-M5	0.058	0.043	0.568	0.837	-
		ANFIS-PSO-M7	0.032	0.026	0.832	0.923	35.28
		ANFIS-ACO-M7	0.055	0.041	0.324	0.692	-12.61
		ANFIS-DE-M5	0.042	0.032	0.623	0.863	16.49
		ANFIS-GA-M5	0.042	0.032	0.599	0.870	15.64
Clear water	Testing	ANFIS-M4	0.116	0.101	0.391	0.750	-
		ANFIS-PSO-M7	0.014	0.012	0.984	0.995	90.09
		ANFIS-ACO-M5	0.053	0.045	0.71	0.909	53.14
		ANFIS-DE-M7	0.090	0.068	0.692	0.846	36.22
		ANFIS-GA-M7	0.087	0.065	0.433	0.789	19.15

Table 11. Performance indices of the best proposed predictive model (ANFIS-PSO-M7) and the models from previous studies

Hydraulic Condition	Phase	Model	RMSE	MAE	R^2	WI
Live bed	Training	Etemad-Shahidi et al. (2011)	0.056	0.044	0.834	0.949
		Sharafati et al. (2018)	0.046	0.034	0.850	0.958
		Present study (ANFIS-PSO-M7)	0.024	0.018	0.957	0.989
	Testing	Etemad-Shahidi et al. (2011)	0.039	0.034	0.688	0.894
		Sharafati et al. (2018)	0.038	0.033	0.798	0.894
		Present study (ANFIS-PSO-M7)	0.032	0.026	0.832	0.923
Clear water	Training	Etemad-Shahidi et al. (2011)	0.121	0.083	0.947	0.931
		Sharafati et al. (2018)	0.071	0.049	0.951	0.982
		Present study (ANFIS-PSO-M7)	0.0048	0.0029	0.999	0.999
	Testing	Etemad-Shahidi et al. (2011)	0.028	0.021	0.962	0.980
		Sharafati et al. (2018)	0.026	0.022	0.973	0.985
		Present study (ANFIS-PSO-M7)	0.014	0.012	0.984	0.995